



Sztukowska, M. N., Ojo, A., Ahmed, S., Carenbauer, A. L., Wang, Q., Shumway, B., Jenkinson, H. F., Wang, H., Darling, D. S., & Lamont, R. J. (2016). Porphyromonas gingivalis initiates a mesenchymal-like transition through ZEB1 in gingival epithelial cells. *Cellular Microbiology*, 18(6), 844-858. <https://doi.org/10.1111/cmi.12554>

Peer reviewed version

License (if available):  
CC BY-NC

Link to published version (if available):  
[10.1111/cmi.12554](https://doi.org/10.1111/cmi.12554)

[Link to publication record in Explore Bristol Research](#)  
PDF-document

This is the author accepted manuscript (AAM). The final published version (version of record) is available online via Wiley at <http://onlinelibrary.wiley.com/doi/10.1111/cmi.12554/abstract>. Please refer to any applicable terms of use of the publisher.

## University of Bristol - Explore Bristol Research

### General rights

This document is made available in accordance with publisher policies. Please cite only the published version using the reference above. Full terms of use are available:  
<http://www.bristol.ac.uk/red/research-policy/pure/user-guides/ebr-terms/>



## Porphyromonas gingivalis Initiates a Mesenchymal-like Transition through ZEB1 in Gingival Epithelial Cells

Journal:	<i>Cellular Microbiology</i>
Manuscript ID	CMI-15-0245.R1
Manuscript Type:	Research article
Date Submitted by the Author:	n/a
Complete List of Authors:	Sztukowska, Maryta; University of Louisville, OIID Ojo, Akintunde; University of Louisville, OIID Ahmed, Saira; University of Louisville, OIID Carenbauer, Anne; University of Louisville, OIID Wang, Qian; University of Louisville, OIID Shumway, Brian; University of Louisville, OIID Jenkinson, Howard; University of Bristol, Oral and dental Sciences Wang, Huizhi; University of Louisville, OIID Darling, Douglas; University of Louisville, OIID Lamont, Richard; University of Louisville Dentistry, Oral Health
Key Words:	Microbial-cell interaction, Disease processes

Revised November 16, 2015

*Porphyromonas gingivalis* Initiates a Mesenchymal-like Transition through ZEB1 in Gingival  
Epithelial Cells

Maryta N. Sztukowska<sup>1</sup>, Akintunde Ojo<sup>1</sup>, Saira Ahmed<sup>1</sup>, Anne L. Carenbauer<sup>1</sup> Qian Wang<sup>1</sup>, Brain  
Shumway<sup>2</sup>, Howard F. Jenkinson<sup>3</sup>, Huizhi Wang<sup>1</sup>, Douglas S. Darling<sup>1</sup>, Richard J. Lamont<sup>1\*</sup>

<sup>1</sup>Department of Oral Immunology and Infectious Diseases, and <sup>2</sup>Department of Surgical and  
Hospital Dentistry, University of Louisville School of Dentistry, Louisville, Kentucky, United  
States of America

<sup>3</sup>School of Oral and Dental Sciences, University of Bristol, Bristol, United Kingdom

\* Corresponding author

570 South Preston Street

University of Louisville

Louisville, KY, 40202

Phone: 502-852-2112

Email: rich.lamont@louisville.edu

Running title: ZEB1 Induction and *P. gingivalis*

## Summary

The oral anaerobe *Porphyromonas gingivalis* is associated with the development of cancers including oral squamous cell carcinoma (OSCC). Here we show that infection of gingival epithelial cells with *P. gingivalis* induces expression and nuclear localization of the ZEB1 transcription factor which controls epithelial-mesenchymal transition (EMT). *P. gingivalis* also caused an increase in ZEB1 expression as a dual species community with *Fusobacterium nucleatum* or *Streptococcus gordonii*. Increased ZEB1 expression was associated with elevated ZEB1 promoter activity and did not require suppression of the miR-200 family of micro RNAs. *P. gingivalis* strains lacking the FimA fimbrial protein were attenuated in their ability to induce ZEB1 expression. ZEB1 levels correlated with an increase in expression of mesenchymal markers, including vimentin and MMP-9, and with enhanced migration of epithelial cells into matrigel. Knockdown of ZEB1 with siRNA prevented the *P. gingivalis*-induced increase in mesenchymal markers and epithelial cell migration. Oral infection of mice by *P. gingivalis* increased ZEB1 levels in gingival tissues, and intracellular *P. gingivalis* were detected by antibody staining in biopsy samples from OSCC. These findings indicate that FimA-driven ZEB1 expression could provide a mechanistic basis for a *P. gingivalis* contribution to OSCC.

19     **Introduction**

20     Once considered implausible, the concept that bacteria can be associated with cancer  
21     development is now well established. Indeed, a causal relationship between *Helicobacter pylori*  
22     and gastric cancer has been demonstrated (Kim *et al.*, 2011), and a growing body of evidence  
23     supports the relationship between specific bacteria and various types of cancer (Garrett, 2015,  
24     Sahingur and Yeudall, 2015). For example, *Fusobacterium nucleatum*, a common inhabitant of  
25     the oral cavity, is over-represented in colorectal carcinoma (Castellarin *et al.*, 2012, Kostic *et al.*,  
26     2012) and can induce colorectal carcinogenesis by activating E-cadherin/ $\beta$ -catenin signaling  
27     (Rubinstein *et al.*, 2013). *F. nucleatum* can also inhibit natural killer (NK) cell cytotoxicity and  
28     killing of various tumors (Gur *et al.*, 2015). High levels of antibodies to *Porphyromonas*  
29     *gingivalis*, a keystone pathogen in periodontal diseases, correlate with a greater than 2-fold  
30     increased risk of pancreatic cancer (Michaud, 2013). *P. gingivalis* is also associated with oral  
31     squamous cell carcinoma (OSCC). The surfaces of OSCCs harbor higher levels of *Porphyromonas*  
32     compared to contiguous healthy mucosa (Nagy *et al.*, 1998), and *P. gingivalis* can be detected  
33     within gingival carcinomas by immunohistochemistry (Katz *et al.*, 2011). Moreover, recent  
34     studies have established that combined infection with *P. gingivalis* and *F. nucleatum* promotes  
35     tumor progression in an oral-specific chemical carcinogenesis mouse model (Gallimidi *et al.*,  
36     2015).

37  
38     *P. gingivalis* and oral epithelial cells engage in an intricate molecular dialog, one consequence  
39     of which is entry of bacterial cells into the cytoplasm of the host cell (Lamont and Hajishengallis,  
40     2015, Lamont *et al.*, 1995). Primary cultures of epithelial cells containing *P. gingivalis* do not

1  
2  
3  
4 41 undergo apoptotic cell death and indeed *P. gingivalis* can suppress several proapoptotic  
5  
6 42 pathways. In response to *P. gingivalis* infection Jak1/Akt/Stat3 signaling is activated with  
7  
8 43 resultant increase in Bcl2 and inhibition of intrinsic mitochondrial apoptotic pathways (Yilmaz *et*  
9  
10 44 *al.*, 2004, Mao *et al.*, 2007). By an independent mechanism *P. gingivalis* upregulates the level  
11  
12 45 of miR-203 which suppresses expression of SOCS3, consequently impeding apoptosis (Moffatt  
13  
14 46 and Lamont, 2011). In tandem with suppression of apoptosis, *P. gingivalis* promotes  
15  
16 47 acceleration of primary epithelial cells through the S-phase of the cell cycle by impacting  
17  
18 48 cyclin/CDK activities and reducing the amount of p53 (Kuboniwa *et al.*, 2008). The process is  
19  
20 49 dependent on the major fimbriae of *P. gingivalis* as a mutant deficient in FimA, the structural  
21  
22 50 fimbrial subunit protein, does not induce increased cell proliferation.  
23  
24  
25  
26  
27  
28  
29  
30

31 51  
32  
33 52 While inhibition of apoptosis and enhanced replication of cells can contribute directly to tumor  
34  
35 53 development, it is unknown if *P. gingivalis* is capable of initiating the malignant transformation  
36  
37 54 or oncogenic progression of epithelial cells. The epithelial-mesenchymal transition (EMT) is a  
38  
39 55 process by which epithelial cells change shape and acquire a motile phenotype (Lamouille *et al.*,  
40  
41 56 2014). The EMT is required for normal development and wound healing; however, it is also  
42  
43 57 associated with the generation of self-renewing tumor-initiating cells, and in a malignant tumor  
44  
45 58 it gives rise to a population of migratory and invasive cancer cells (Lamouille *et al.*, 2014). This  
46  
47 59 switch in cell differentiation and behavior is controlled by a group of transcription factors  
48  
49 60 including the zinc-finger E-box-binding homeobox 1 and 2 proteins (ZEB1/2), SNAIL and TWIST  
50  
51 61 (Vandewalle *et al.*, 2009, Scanlon *et al.*, 2013). The ZEB1 ( $\delta$ EF1, Zfhx1a, Zfhx1b) and ZEB2 (SIP1)  
52  
53 62 transcription factors are critical EMT activators that bind to 5'-CACCTG sequences and repress  
54  
55  
56  
57  
58  
59  
60

transcription of epithelial specific genes such as E-cadherin (*cdh1*) (Vandewalle *et al.*, 2009). ZEB can also positively regulate genes associated with the mesenchymal phenotype such as those encoding vimentin and matrix-metalloproteinases (Vandewalle *et al.*, 2009, Lamouille *et al.*, 2014). ZEB1/2 are in the TGF $\beta$  signaling pathway, binding SMADs and having essential effects on embryonic development (Gheldof *et al.*, 2012). ZEB1 has been implicated in activating EMT and metastasis in several type of cancers (Sanchez-Tillo *et al.*, 2012, Jia *et al.*, 2012). Moreover, ZEB1/2 are linked to the miR-200 family in a reciprocal negative feedback loop whereby each regulates the expression of the other (Brabletz and Brabletz, 2010).

*H. pylori* has been shown to upregulate expression of ZEB1 which can initiate an EMT and cancer stem-cell properties in infected gastric epithelial cells (Baud *et al.*, 2013, Bessede *et al.*, 2014). In this study we show that *P. gingivalis* can increase ZEB1 levels in gingival epithelial cells in a fimbriae dependent manner. Upregulation of *ZEB1* was dependent on increased promoter activity. Elevated expression of ZEB1 was associated with a **partial** mesenchymal phenotype in *P. gingivalis*-infected gingival epithelial cells, including increased migration. We also detected *P. gingivalis* antigens in oral carcinoma in situ and poorly differentiated cancer, and mice orally infected with *P. gingivalis* had an increase in ZEB1 mRNA expression in gingival tissues. The results suggest a novel mechanism by which oral bacteria such as *P. gingivalis* can contribute to a mesenchymal phenotype, and potentially drive the progression of cancer.

**Results**

***P. gingivalis* upregulates ZEB1 in gingival epithelial eells**

We investigated the impact of *P. gingivalis* on ZEB1 expression in TIGK cells using qRT-PCR and immunoblotting. As shown in Figure 1A, *P. gingivalis* increased ZEB1 mRNA levels in a time and dose dependent manner, with maximal induction occurring after 24 h infection with a MOI of 100. An increase in the amount of ZEB1 protein was also observed at 24 h following *P. gingivalis* infection at both MOI 50 and 100 (Fig 1B). As *P. gingivalis* infections of oral tissue are chronic conditions, we further examined ZEB1 activity 72 h after *P. gingivalis* infection. MOIs of 1, 10 and 50 were used as at MOI 100 the proteases of *P. gingivalis* can cause detachment of cells from the substratum. While an MOI 1 did not affect ZEB1 expression, mRNA levels were increased by *P. gingivalis* at MOI 10 and 50 (Figure 1C). The ability of *P. gingivalis* at MOI 10 to increase ZEB1 expression after 72 h, but not earlier, indicates that infection of epithelial cells with low numbers of the organism has the potential to elevate ZEB1 over extended times, possibly as a result of intracellular *P. gingivalis* replication and cell to cell spread (Lamont *et al.*, 1995, Yilmaz *et al.*, 2006). To corroborate the nuclear location of the ZEB1 transcription factor following *P. gingivalis* infections, TIGKs were examined by CLSM with quantitative image analysis (Figures 1D and E). After *P. gingivalis* infection there was increased expression of ZEB1 protein in the nucleus where it is functionally active.

#### **ZEB1 responses to *P. gingivalis* are strain and fimbriae dependent**

*P. gingivalis* is a host adapted organism with a nonclonal population structure, and isolates from different individuals often vary considerably (Tribble *et al.*, 2013). Hence, we next examined the ability of different strains of *P. gingivalis* to enhance ZEB1 mRNA levels. As shown in Figure 1F, an additional ATCC strain (49417) and two low passage clinical isolates (11029 and



1  
2  
3 107 10512) induced *ZEB1* expression to a similar degree as the type strain 33277. In contrast, the  
4  
5  
6 108 commonly used laboratory strain W83 did not significantly increase *ZEB1* expression. One of  
7  
8  
9 109 the major differences among *P. gingivalis* strains is in the expression of fimbriae (Nadkarni *et*  
10  
11 110 *al.*, 2014). The two ATCC strains, along with the two low passage isolates, all expressed FimA,  
12  
13 111 the structural subunit protein of the major fimbriae (Supporting Information Figure S1). Strain  
14  
15  
16 112 W83 does not express FimA (Nishikawa and Duncan, 2010), which prompted us to speculate  
17  
18  
19 113 that FimA may be an effector protein for *ZEB1* induction. This concept was corroborated by the  
20  
21 114 failure of an isogenic *fimA* mutant of 33277 to increase *ZEB1* mRNA levels (Figure 1G). We also  
22  
23  
24 115 found that induction of *ZEB1* expression required direct contact between *P. gingivalis* and  
25  
26 116 epithelial cells (Figure 1G), consistent with a role for the FimA adhesin. Fimbriated *P. gingivalis*  
27  
28  
29 117 activate JNK signaling (Watanabe *et al.*, 2001) which has been reported to increase  
30  
31 118 transcription of *ZEB1* (Zhang *et al.*, 2012). However, siRNA knockdown of JNK in TIGK cells did  
32  
33  
34 119 not impede the ability of *P. gingivalis* to upregulate *ZEB1* (Supporting Information Figure S2). In  
35  
36 120 addition, pharmacological inhibition of Akt with LY294002 also failed to reduce *P. gingivalis*-  
37  
38  
39 121 mediated *ZEB1* induction (Supporting Information Figure S3). Hence the signaling pathways  
40  
41 122 activated by *P. gingivalis* fimbriae that converge on *Zeb1* remain to be determined, and this  
42  
43  
44 123 topic is under active investigation in our laboratory.  
45  
46 124  
47  
48  
49 125 The FimA fimbriae are required for maximal invasion of *P. gingivalis* into gingival epithelial cells  
50  
51 126 (Lamont and Jenkinson, 1998). However, invasion per se was not required for *ZEB1* induction  
52  
53  
54 127 as a mutant of *P. gingivalis* that is invasion-deficient, due to disruption of the gene encoding the  
55  
56 128 serine phosphatase SerB (Takeuchi *et al.*, 2013), retained the ability to upregulate *ZEB1*  
57  
58  
59  
60

(Supporting Information Figure S4). Nonetheless, the spatial definition of *P. gingivalis* initiation of ZEB1 activation requires further study. Moreover, when *P. gingivalis* was separated from the epithelial cells by a semi-permeable membrane, *ZEB1* levels were lower than the control uninfected condition, indicating that there may be components secreted by *P. gingivalis* that can antagonize *ZEB1* regulation in the absence of FimA mediated contact. Thus, multiple effectors of *P. gingivalis* may be capable of impacting *ZEB1* expression, with the effect of whole cells representing the collective output of several distinct interactions and signaling pathways.

### ***P. gingivalis* communities regulate ZEB1 expression**

On mucosal surfaces bacteria rarely exist as monospecies accumulations but rather as complex multispecies communities. *P. gingivalis* engages in synergistic community formation with *S. gordonii* and *F. nucleatum*, common inhabitants of the oral microbiota, and *in vivo* these organisms can be found in close association (Benitez-Paez *et al.*, 2014, Valm *et al.*, 2011, Wright *et al.*, 2014, Hendrickson *et al.*, 2014). Individually, neither *S. gordonii* nor *F. nucleatum* were capable of regulating ZEB1 expression, indicating that of these three widespread oral species, *P. gingivalis* has the most potential to effect an EMT through ZEB1 (Figure 2). Importantly, *P. gingivalis* remained effective at elevating ZEB1 mRNA in the context of a community with either *S. gordonii* or *F. nucleatum*, consistent with recent reports demonstrating that a community of *P. gingivalis* and *F. nucleatum* can promote tumor progression in animal models (Gallimidi *et al.*, 2015). Thus, the tumorigenic properties of *P. gingivalis* can prevail in the presence of co-colonizing organisms, an important principle for *in vivo* relevance.

1  
2  
3  
4  
5  
6  
7  
8  
9  
10  
11  
12  
13  
14  
15  
16  
17  
18  
19  
20  
21  
22  
23  
24  
25  
26  
27  
28  
29  
30  
31  
32  
33  
34  
35  
36  
37  
38  
39  
40  
41  
42  
43  
44  
45  
46  
47  
48  
49  
50  
51  
52  
53  
54  
55  
56  
57  
58  
59  
60

***P. gingivalis* upregulates ZEB1 promoter activity and downregulates miR200**

An increase in the amount of steady state mRNA levels can result from an increase in transcription or a decrease in degradation. To begin to distinguish between these possibilities, we first examined transcriptional activity from the *ZEB1* promoter using a series of *ZEB1* upstream regulatory regions promoting transcription of the *luc* gene. These human *ZEB1* promoter constructs contain sequences important for regulation of ZEB1 expression in several cell types (Manavella *et al.*, 2007, Liu *et al.*, 2007). *P. gingivalis* stimulated the activity of all of these promoter constructs (Figure 3A), indicating that the increase of ZEB1 mRNA induced by *P. gingivalis* can occur through an elevated transcription rate. These data also localize the response element(s) within the first 400 bp of the promoter. An additional mechanism by which ZEB1 is controlled posttranscriptionally is through the action of the miR-200 family of microRNAs (Brabletz and Brabletz, 2010). miR-200 family members target conserved recognition sites on the 3' UTR of ZEB1 mRNA (Brabletz and Brabletz, 2010), and thus a decrease in miR-200 leads to higher levels of ZEB1 mRNA. However, we did not observe a reduction in the amount of miR-200b, miR-200c or miR-205 in cells at 6 h after *P. gingivalis* infection when levels of ZEB1 mRNA begin to rise (Figure 3B-D). Indeed there was a slight increase in miR-200 family expression, indicating that the increase in ZEB1 levels at 6 h is not the consequence of decreased miR-200 expression. The action of ZEB1, in turn, represses the transcription of the miR-200 family, and consistent with this at 24 and 48 h after *P. gingivalis* infection, miR-200b, miR-200c and miR-205 levels were reduced. A control microRNA, miR-21, which is not involved in *ZEB1* feedback regulation, did not show a significant decrease in expression (Supporting Information Figure S5). Hence, the pattern of miRNA expression is

consistent with the results from the promoter-reporter constructs in pointing toward increased mRNA synthesis as the initial cause of the elevated levels of steady state mRNA for ZEB1.

### Changes in epithelial and mesenchymal marker expression upon *P. gingivalis* infection

The expression pattern of ZEB1 targets in TIGKs infected with *P. gingivalis* was assessed by qRT-PCR (Table 1). Mesenchymal markers N-cadherin, vimentin and matrix metalloproteinase (MMP)-9 were upregulated at 24 h after infection by *P. gingivalis* at MOI 50 and 100, while fibronectin levels were increased by *P. gingivalis* at MOI 100. An increase in vimentin protein expression was confirmed by immunoblotting (Supporting Information Figure S6), and elevated MMP-9 amounts following infection with fimbriated *P. gingivalis* was corroborated by zymography (Figure 4). While both pro and active forms of MMP-9 were increased by *P. gingivalis* wild type, there was no difference in the ratio of active MMP-9 to total (cleaved and pro-MMP9) between parental and fimbrial deficient mutant strains. Under these infection conditions, therefore, fimbriated *P. gingivalis* elevate the amount of MMP-9 produced by TIGK cells but do not modulate MMP-9 activation. In contrast expression of MMP-2, which may be more predominantly regulated by Twist (Yang *et al.*, 2013), was not impacted by *P. gingivalis* infection. Of the epithelial markers tested, collagen 1 (COL1A1) and cytokeratin 19 (KRT19) were suppressed by *P. gingivalis*. Collectively, these results support the concept that infection by *P. gingivalis* can contribute to the process of transition toward a mesenchymal phenotype.

Although the mesenchymal marker integrin  $\alpha 5$  (ITGA5) and the epithelial marker cytokeratin 7 (KRT7) were unaffected by *P. gingivalis*, variability in expression of important cell proteins is not unexpected as control of expression by ZEB1 is cell and context dependent (Lamouille *et al.*,

1  
2  
3  
4  
5  
6  
7  
8  
9  
10  
11  
12  
13  
14  
15  
16  
17  
18  
19  
20  
21  
22  
23  
24  
25  
26  
27  
28  
29  
30  
31  
32  
33  
34  
35  
36  
37  
38  
39  
40  
41  
42  
43  
44  
45  
46  
47  
48  
49  
50  
51  
52  
53  
54  
55  
56  
57  
58  
59  
60

2014). One of the major targets of ZEB1 is E-cadherin, and ZEB1 mediated repression of E-cadherin, with associated disruption of E-cadherin dependent junctions, is an important marker of EMT. We did not observe differential regulation of E-cadherin following *P. gingivalis* infection (not shown). However, the gingival epithelium is highly porous with only sparse interconnections (Bosshardt and Lang, 2005) and expression of E-cadherin is very low (Heymann *et al.*, 2001). Thus a reduction of E-cadherin may not be as important for the EMT of gingival epithelial cells as in other cell types.

To corroborate the role ZEB1 in the differential regulation of mesenchymal markers, siRNA mediated knockdown was performed. Reduction of ZEB1 mRNA and protein following siRNA transfection was confirmed by qRT-PCR and immunoblotting, respectively (Figure 5A,B). TIGKs with diminished ZEB1 expression were then infected with *P. gingivalis* MOI 50 or 100 over 24 h. As shown in Figure 5C and D, ZEB1 deficiency prevented *P. gingivalis* induced modulation of expression of vimentin and MMP-9.

***P. gingivalis* promotes migration of epithelial cells**

Cells that acquire an EMT phenotype display an invasive behavior *in vitro*, and thus we tested the ability of *P. gingivalis* to increase the migration of TIGK cells into matrigel. Figure 6 shows that *P. gingivalis* infection resulted in a greater than 2-fold increase in TIGK cell invasion into the gel compared to control cells. Knockdown of ZEB1 prevented *P. gingivalis*-induced TIGK cell migration, verifying the importance of ZEB1 in this aspect of the *P. gingivalis*-dependent partial mesenchymal phenotype.

217

**218 *P. gingivalis* elevates ZEB1 levels *in vivo***

219 To determine whether *P. gingivalis*' ability to increase ZEB1 levels also occurs *in vivo*, mice were  
220 orally infected with *P. gingivalis*, and gingival tissue recovered 1, 3 and 8 days following the final  
221 inoculation. Levels of *P. gingivalis* on the gingival tissues were determined by qPCR (Supporting  
222 Information Figure S7) and remained constant over the 8-day period. As shown in Figure 7,  
223 colonization with *P. gingivalis* induced an increase in gingival tissue expression of ZEB1 mRNA  
224 over 8 days compared to sham infected animals. Thus, *P. gingivalis* has the potential to  
225 stimulate ZEB1 and contribute to an EMT in an animal model.

226

**227 Presence of *P. gingivalis* in human OSCC**

228 *P. gingivalis* could exacerbate carcinogenesis at several stages through its ability to increase  
229 ZEB1 expression, but only if the bacteria are physically associated with the developing cancer.  
230 We investigated whether *P. gingivalis* bacteria are present within oral squamous cell carcinoma  
231 biopsy samples. Immunofluorescence microscopy with a specific polyclonal *P. gingivalis*  
232 antiserum labeled discrete speckles in the cells of a poorly differentiated OSCC sample and a  
233 carcinoma in situ, whereas antibodies to *S. gordonii* showed little or no labeling (Figure 8A-B).  
234 Similar results were seen with two carcinoma in situ cases and two poorly differentiated  
235 carcinomas. Confocal microscopy more clearly detected the particles which were fluorescently  
236 labeled by the *P. gingivalis* antibodies. Serial optical sections were taken at 0.4 microns, and  
237 individual particles were found to persist in 5 to 7 adjacent optical slices (Supporting  
238 Information Figure S8). This estimates the fluorescent particles to be 2.0 to 2.8 microns in size,

1  
2  
3  
4  
5  
6  
7  
8  
9  
10  
11  
12  
13  
14  
15  
16  
17  
18  
19  
20  
21  
22  
23  
24  
25  
26  
27  
28  
29  
30  
31  
32  
33  
34  
35  
36  
37  
38  
39  
40  
41  
42  
43  
44  
45  
46  
47  
48  
49  
50  
51  
52  
53  
54  
55  
56  
57  
58  
59  
60

239 consistent with intact *P. gingivalis*. As described in primary gingival epithelial cells, *P. gingivalis*  
240 was observed in both the cytoplasm and in the nuclei (Belton *et al.*, 1999).

241  
242 **Discussion**

243 Typically, the gingival epithelium provides a major physical barrier to oral pathogens. Disruption  
244 of the gingival barrier by inducing an EMT may enhance the ability of *P. gingivalis* to invade the  
245 tissue and enhance access to nutrients derived from inflammatory tissue breakdown  
246 (Hajishengallis, 2014). Hence, up-regulation of ZEB1 by *P. gingivalis* can be seen as providing an  
247 evolutionary advantage to the organism. Beyond this, the ability of *P. gingivalis* to stimulate  
248 ZEB1 expression could have several distinct clinically relevant effects. ZEB1 influences multiple  
249 stages of carcinogenesis, including the initial transformation, progression, EMT leading to  
250 metastasis, and resistance to therapy (Sanchez-Tillo *et al.*, 2012, Zhang *et al.*, 2014). Therefore,  
251 the presence of *P. gingivalis*, interacting with other environmental effectors, may enhance the  
252 initiation of oral cancer within the pre-cancerous field, or increase carcinogenic progression.

253  
254 The ability to manipulate ZEB1 location and function constitutes an important attribute of  
255 bacteria with a potential role in carcinogenesis. *P. gingivalis* is a keystone member of dysbiotic  
256 oral communities, which in combination with its ability to spread systemically, and enhance cell  
257 survival and proliferation, supports epidemiological evidence of an association with cancers  
258 such as OSCC (Whitmore and Lamont, 2014, Lamont and Hajishengallis, 2015). Moreover, in  
259 established invasive OSCC lines, *P. gingivalis* activates the ERK1/2-Ets1, p38/HSP27, and  
260 PAR2/NF-κB pathways to promote cellular invasion (Inaba *et al.*, 2014). The results of the

present study indicate the *P. gingivalis* may induce nontransformed gingival epithelial cells to undergo a partial EMT through the upregulation of ZEB1. We show that *P. gingivalis* increases the transcriptional activity of the ZEB1 gene and increases ZEB1 protein levels in the nucleus. Infection of epithelial cells with *P. gingivalis* upregulated expression of genes associated with the mesenchymal phenotype and knockdown of ZEB1 attenuated this effect. *P. gingivalis* also induced a migratory phenotype in epithelial cells which was ZEB1-dependent. Oral infection of mice with *P. gingivalis* stimulated ZEB1 expression in the gingival tissues and biopsy tissue from human OSCC carcinoma in situ and poorly differentiated cancer showed the presence of *P. gingivalis*.

On the hard and soft tissues of the oral cavity *P. gingivalis* is an inhabitant of multispecies communities. Organisms such as *S. gordonii* and *F. nucleatum* provide mutual physiological support, and *P. gingivalis* in the context of a community is phenotypically distinct from single species accumulations (Wright *et al.*, 2013). In addition, infection of epithelial cells with the early colonizing streptococci can reprogram specific signaling pathways such that they do not respond to the later colonizing *P. gingivalis* (Handfield *et al.*, 2005). We found here that while neither *S. gordonii* nor *F. nucleatum* modulated ZEB1 mRNA levels, combinations of *P. gingivalis* with either species retained the capacity to upregulate ZEB1. As porphyromonads, fusobacteria and streptococci are all found in higher numbers on the surfaces of OSCC compared to contiguous healthy mucosa (Nagy *et al.*, 1998), it is likely therefore that these microbial communities contribute to the EMT.



1  
2  
3 283 *P. gingivalis* strains exhibit extensive genetic variation as a result of genomic rearrangements  
4  
5  
6 284 (Naito *et al.*, 2008), and horizontal gene transfer is considered an adaptive strategy for long  
7  
8  
9 285 term survival in the oral environment (Nadkarni *et al.*, 2014, Tribble *et al.*, 2007). Most strains  
10  
11 286 of *P. gingivalis* expresses fimbriae comprised of FimA major fimbrial subunit proteins, although  
12  
13  
14 287 in some strains, such as the commonly used lab strain W83, FimA production is very low due to  
15  
16 288 a mutation in the FimS histidine kinase component of the FimS/FimR TCS that controls  
17  
18  
19 289 transcription of the *fimA* operon (Nishikawa and Duncan, 2010). Results with a variety of strains  
20  
21 290 and isogenic mutants of *P. gingivalis* indicate that FimA is the effector of *P. gingivalis*  
22  
23  
24 291 responsible for upregulation of ZEB1. FimA is a major antigen on the *P. gingivalis* surface and  
25  
26 292 can also incite the production of proinflammatory cytokines (Lamont and Jenkinson, 1998,  
27  
28 293 Bostanci and Belibasakis, 2012). FimA is capable of manipulating a number of signal  
29  
30  
31 294 transduction pathways and transcription factors in different cell types (Zhou and Amar, 2007,  
32  
33  
34 295 Hajishengallis *et al.*, 2012), and the processes that lead to increased ZEB1 promoter activity  
35  
36 296 require further study. The potential importance of FimA expressing *P. gingivalis* lineages in the  
37  
38  
39 297 events that can lead to tumor development is corroborated by the role of this protein in the  
40  
41 298 acceleration of the epithelial cell cycle (Kuboniwa *et al.*, 2008). FimA fimbriae, which do not  
42  
43  
44 299 share significant homology to other fimbrial proteins (Enersen *et al.*, 2013), may thus constitute  
45  
46 300 an attractive target for novel biomarkers or therapeutics.  
47  
48  
49 301  
50  
51 302 ZEB1 can be regulated at the transcriptional level and posttranscriptionally regulated by the  
52  
53  
54 303 miR-200 family through a double negative feedback loop (Brabletz and Brabletz, 2010). In  
55  
56 304 epithelial cells miR-200s inhibit ZEB expression and maintain the epithelial phenotype. By  
57  
58  
59  
60

1  
2  
3 305 contrast, in mesenchymal cells elevated ZEB activity suppresses expression of the miR-200s.  
4  
5  
6 306 Our results show that the increased levels of ZEB1 were associated with a reduction in the  
7  
8  
9 307 amounts of the miR200 family, potentially facilitating a stable transition to the **partial**  
10  
11 308 mesenchymal phenotype. The initial upregulation of *ZEB1* in epithelial cells, however, was not  
12  
13  
14 309 associated with a decrease in the amounts of the miR200 family, but with an increase in ZEB1  
15  
16 310 promoter activity. NF- $\kappa$ B activation also promotes ZEB1 transcription (Vandewalle *et al.*, 2009);  
17  
18  
19 311 however, in epithelial cells *P. gingivalis* suppresses the activation of NF- $\kappa$ B by  
20  
21 312 dephosphorylation of the p65 subunit at the S536 residue (Takeuchi *et al.*, 2013). It is unlikely,  
22  
23  
24 313 therefore, that NF- $\kappa$ B is involved in *P. gingivalis*-induced ZEB1 upregulation.  
25  
26 314

27  
28 315 *P. gingivalis* induced expression of the mesenchymal markers and decreased expression of the  
29  
30  
31 316 epithelial markers. siRNA knockdown of ZEB1 abrogated the ability of *P. gingivalis* to regulate  
32  
33  
34 317 epithelial and mesenchymal gene expression, establishing ZEB1 as a major transcriptional  
35  
36 318 effector of the *P. gingivalis*-induced **partial** EMT. **Epithelial markers down regulated by *P.***  
37  
38 319 ***gingivalis* included cytokeratin 19 which is characteristically expressed in cells of the junctional**  
39  
40  
41 320 **epithelium within the gingival tissues, and has also been reported to be suppressed in OSCC**  
42  
43  
44 321 **(Khanom *et al.*, 2012).** The mesenchymal relevant genes induced by *P. gingivalis* included **N-**  
45  
46 322 **cadherin**, vimentin, fibronectin and MMP-9. **N-cadherin is a calcium dependent cell-cell**  
47  
48  
49 323 **adhesion glycoprotein, which is upregulated in EMT and some studies have found associated**  
50  
51 324 **with OSCC (Zhao *et al.*, 2012).** Vimentin is a cytoskeletal intermediate filament protein involved  
52  
53  
54 325 in maintaining cell shape and stabilizing cytoskeletal interactions. Expression of vimentin is  
55  
56 326 associated with OSCC tumorigenesis (Lee *et al.*, 2015), and vimentin has been proposed as a  
57  
58  
59  
60

1  
2  
3  
4  
5  
6  
7  
8  
9  
10  
11  
12  
13  
14  
15  
16  
17  
18  
19  
20  
21  
22  
23  
24  
25  
26  
27  
28  
29  
30  
31  
32  
33  
34  
35  
36  
37  
38  
39  
40  
41  
42  
43  
44  
45  
46  
47  
48  
49  
50  
51  
52  
53  
54  
55  
56  
57  
58  
59  
60

327 predictor of the malignant potential of high risk oral lesions (Sawant *et al.*, 2014). Fibronectin is  
328 a component of the cell matrix involved in cell migration processes including metastasis, and  
329 expression of alternatively spliced segments of fibronectin is related to OSCC tumorigenesis  
330 (Kamarajan *et al.*, 2010). MMP-9 is secreted as inactive proproteins which are activated by  
331 proteolytic cleavage. As a gelatinase, MMP-9 can degrade collagen IV in the basement  
332 membrane and extracellular matrix facilitating tumor growth, invasion, metastasis, and  
333 angiogenesis (Westermarck and Kahari, 1999). MMP-9 plays a crucial role in the development  
334 of several human malignancies, including OSCC (Kruger *et al.*, 2005, Bedal *et al.*, 2014).  
335 Moreover, epithelial cells infected with *P. gingivalis* showed ZEB1-dependent increased  
336 migration into matrigel, a phenotype consistent with increased MMP-9 activity and with an  
337 overall **partial** mesenchymal phenotype.

338  
339 To begin to translate our results from reductionist *in vitro* models to the *in vivo* situation, we  
340 orally infected mice with *P. gingivalis* and examined ZEB1 expression in gingival tissues.  
341 Although *P. gingivalis* is not a normal member of the mouse oral microbiota, it does colonize  
342 transiently and causes alveolar bone loss (Hajishengallis *et al.*, 2015). Our results show for the  
343 first time that *P. gingivalis* colonization of the gingival tissues *in vivo* leads to upregulation of  
344 ZEB1. Further *in vivo* evidence for a role of *P. gingivalis* in oral tumor development was  
345 provided by IF analysis of OSCC biopsy samples. Antigenic based detection of *P. gingivalis* within  
346 biopsy samples from OSCC poorly differentiated cancer and carcinoma in situ corroborates a  
347 similar study in which *P. gingivalis* antigens were detected in ten gingival squamous cell  
348 carcinomas of differing degrees of differentiation (Katz *et al.*, 2011). The use of optical

sectioning in the current study established that the size of particles detected by *P. gingivalis* antibodies was in the 2-3  $\mu\text{m}$  range, consistent with whole organisms, rather than shed antigens or outer membrane vesicles. Intimate association of *P. gingivalis* with OSCC lesions shows that the organism has the opportunity as well as the capability, to contribute to EMT *in vivo*.

Oral cancers are among the most prevalent (Jemal *et al.*, 2008), and despite considerable advances in diagnosis and therapeutic options, the 5-year survival rate has remained stable at approximately 50% among all tumor stages during the past decades (Wikner *et al.*, 2014). The early phase of OSCC is often asymptomatic, therefore the identification of both novel biomarkers and contributing etiological agents is important for improving survival rates. The results of the current study suggest that infection with FimA-positive *P. gingivalis* can induce a ZEB1 dependent **partial** EMT. The detection of *P. gingivalis*, or of FimA, in early erythroplakia or leukoplakia lesions, therefore, may have utility for the early detection of lesion likely to progress to malignant status.

## Materials and Methods

### Bacterial strains, eukaryotic cells, and growth and infection conditions

*Porphyromonas gingivalis* strain ATCC 33277 and its isogenic mutant  $\Delta\text{fimA}$ , strains ATCC 49417, W83, and low passage clinical isolates 11029, 10512 (laboratory strains), were cultured in trypticase soy broth (TSB) supplemented with yeast extract (1 mg/ml), hemin (5  $\mu\text{g}/\text{ml}$ ) and menadione (1  $\mu\text{g}/\text{ml}$ ). Tetracycline (1  $\mu\text{g}/\text{ml}$ ) was incorporated into the medium for the growth

1  
2  
3  
4  
5  
6  
7  
8  
9  
10  
11  
12  
13  
14  
15  
16  
17  
18  
19  
20  
21  
22  
23  
24  
25  
26  
27  
28  
29  
30  
31  
32  
33  
34  
35  
36  
37  
38  
39  
40  
41  
42  
43  
44  
45  
46  
47  
48  
49  
50  
51  
52  
53  
54  
55  
56  
57  
58  
59  
60

of  $\Delta fimA$ . *Fusobacterium nucleatum* ATCC 25586 was cultured in brain heart infusion (BHI) broth supplemented with hemin (5  $\mu\text{g/ml}$ ) and menadione (1  $\mu\text{g/ml}$ ). *Streptococcus gordonii* DL1 was grown in BHI supplemented with yeast extract (5  $\mu\text{g/ml}$ ). All bacterial strains were cultured anaerobically at 37°C. Human telomerase immortalized keratinocytes (TIGKs) derived from gingival epithelium were maintained at 37°C and 5% CO<sub>2</sub> in Dermalife-K serum free culture medium (Lifeline Cell Technology, Carlsbad, CA) as described (Moffatt-Jauregui *et al.*, 2013). TIGKs between passages 10 and 20 at 70% confluence were stimulated with bacteria as described for individual experiments. For transwell (Corning, Corning NY) assays, TIGKs were cultured in the lower compartment and *P. gingivalis* added to the upper chamber.

**Immunoblotting**

TIGK cells were solubilized in cold cell lysis reagent (Cell Signaling, Danvers, MA) containing Protease Inhibitor and PhosSTOP Phosphatase Inhibitor (Roche, Indianapolis, IN). Proteins (40 ng) were separated by 10% SDS-polyacrylamide gel electrophoresis, blotted onto a PVDF membrane and blocked in 5% BSA in TBS with 0.1% Tween20. Blots were probed at 4°C overnight with primary antibodies followed by 1 h with HRP-conjugated secondary antibody at room temperature. Antigen-antibody binding were detected using ECL Substrate (Thermoscientific, Hudson NH). Primary antibodies targeted ZEB1 (Novus, Littleton, CO) or vimentin (Cell Signaling). Duplicate blots were probed with GAPDH antibodies (Cell Signaling) as a loading control

**RNA extraction and quantitative reverse transcription-PCR (qRT-PCR)**

1  
2  
3 392 Total RNA from TIGK cells and from homogenized gingival tissue was isolated and purified with  
4  
5  
6 393 PerfectPure RNA kit (5Prime, Gaithersburg, MD). miRNA was isolated and purified from TIGKs  
7  
8  
9 394 with PureLink miRNA isolation kit (Invitrogen, Carlsbad, CA). RNA concentrations were  
10  
11 395 determined by spectrophotometry (NanoDrop Technology, Wilmington, DE). cDNA from total  
12  
13 396 RNA and miRNA was synthesized (2 µg RNA/reaction volume) using a High Capacity cDNA  
14  
15  
16 397 Reverse Transcription kit and a TaqMan MicroRNA Reverse Transcription kit (Applied  
17  
18 398 Biosystems, Grand Island, NY), respectively. Real time RT-PCRs used TaqMan Fast universal PCR  
19  
20  
21 399 mastermix and gene expression assays for Zeb1, vimentin, MMP-9, ITGA5, fibronectin, KRT7,  
22  
23 400 COL-1A1 and GAPDH. Negative RT reactions were included in each assay. TaqMan microRNA  
24  
25  
26 401 assays were used to quantify the mature miRNA-200b, mi-RNA-200c, miRNA-205, miRNA-21  
27  
28 402 and RNU48. Real time qPCR was performed on an Applied Biosystems StepOne Plus cyclor with  
29  
30  
31 403 StepOne software V2.2.2 and autocalculated threshold cycle selected. The cycle threshold ( $C_t$ )  
32  
33 404 values were determined, mRNA and miRNA expression levels were normalized to GAPDH and  
34  
35  
36 405 RNU48, respectively, and expressed relative to controls following the  $2^{-\Delta\Delta C_t}$  method.  
37  
38  
39 406  
40

#### 41 **Luciferase reporter assay**

42  
43 408 TIGK cells were transfected with ZEB1 promoter constructs: Z1p 1000-Luc (-912 bp to +43 bp of  
44  
45  
46 409 the ZEB1 gene), Z1p.400-Luc (-367 bp to +43 bp) and Z1p.196-Luc (-212 bp to +43 bp); at 2  
47  
48 410 µg/10<sup>5</sup> cells using FuGENE6 Transfection Reagent (Promega, Madison, WI). Following 48 h in  
49  
50  
51 411 transfection media, cells were returned to TIGK medium for further 24 h, prior to the  
52  
53  
54 412 stimulation with *P. gingivalis*. Cells were lysed and the reporter activity was determined with  
55  
56  
57  
58  
59  
60

1  
2  
3 413 the Dual-Glo Luciferase Assay System (Promega). Firefly luciferase activity was normalized on  
4  
5  
6 414 the basis of Renilla luciferase activity in the same samples.  
7  
8  
9 415

10  
11 416 **Zymography**

12  
13 417 The activities of MMP2 and MMP9 in culture supernatant collected from control uninfected and  
14  
15  
16 418 *P. gingivalis*-infected TIGK cells, were determined using gelatin zymography as described (Inaba  
17  
18 419 *et al.*, 2014). Samples were mixed with SDS sample buffer without reducing reagents, then  
19  
20  
21 420 separated on 10% SDS-polyacrylamide gels containing 0.1% gelatin. The gels were incubated at  
22  
23 421 37°C with 2.5% Triton X-100 for 1 h, and then in 20 mM Tris-HCl (pH 7.5) containing 200 mM  
24  
25  
26 422 NaCl and 5 mM Ca Cl<sub>2</sub> for 48 h. After staining with 5% Coomassie Brilliant Blue R-250,  
27  
28 423 gelatinolytic activities were visualized as clear bands against a blue background and quantified  
29  
30  
31 424 using ImageJ.  
32  
33  
34 425

35  
36 426 **RNA interference**

37  
38 427 TIGKs were transfected with predesigned 30 nM siRNA (siGENOME SMARTpool siRNA) targeting  
39  
40  
41 428 ZEB1 or control siRNA (GE Healthcare Dharmacon, Lafayette, CO) for 24 h using LipoJet  
42  
43 429 (SignaGen, Gaithersburg, MD) transfection reagent. At 48 h after transfection, the medium was  
44  
45  
46 430 replaced and cells were incubated for a further 24 h prior to infection.  
47  
48  
49 431

50  
51 432 **Immunofluorescence and confocal laser scanning microscopy**

52  
53 433 TIGK cells were grown on glass coverslips, washed twice in phosphate-buffered saline (PBS) and  
54  
55  
56 434 fixed with 4% paraformaldehyde for 10 min. Permeabilization was with 0.2% TritonX-100 for 10  
57  
58  
59  
60

1  
2  
3 435 min at room temperature prior to blocking in 10% goat serum for 20 min. ZEB1 was detected by  
4  
5  
6 436 reacting with primary antibodies at 1:100 overnight at 4°C, followed by Alexa Fluor 488-  
7  
8  
9 437 conjugated anti-rabbit secondary antibodies (Life Technologies) at 1:200 for 3 h in the dark.  
10  
11 438 Following a 20 min blocking in 0.1% goat serum, actin was labeled with Texas Red-phalloidin  
12  
13 439 (Life Technologies) for 2 h at room temperature in the dark. Coverslips were mounted with on  
14  
15  
16 440 glass slides using ProLong Gold with DAPI (4'-diamidino-2-phenylindole) mounting medium  
17  
18 441 (Invitrogen) prior to imaging with a Leica SP8 confocal inverted fluorescence microscope.  
19  
20  
21 442 Images were analyzed using Volocity 6.3 Software (PerkinElmer, Waltham, MA).  
22  
23  
24 443  
25

#### 26 444 **Matrigel invasion assay**

27  
28 445 Cell motility was measured by assessment of the migration rate of TIGKs using a BD BioCoat  
29  
30  
31 446 Matrigel Invasion Chamber (BD Biosciences, San Jose, CA). Cells ( $2 \times 10^5$ ) were plated on  
32  
33  
34 447 transwell filters coated with matrigel. The lower compartment of the invasion chambers  
35  
36 448 contained cell culture medium. After 18 h incubation at 37°C, cells remaining on the upper  
37  
38 449 surface of the filter were removed, and the cells that migrated through the filter were fixed  
39  
40  
41 450 with 1% methanol and stained with toluidine blue. Cells were enumerated from three random  
42  
43  
44 451 20X fields for each filter using a Nikon Eclipse TS100 microscope.  
45  
46  
47 452  
48

#### 49 453 **Animal infection**

50  
51 454 BALB/c mice were orally infected with  $10^7$  cfu *P. gingivalis* 33277 five times at 2-day intervals as  
52  
53  
54 455 described previously (Daep *et al.*, 2011) and approved by the University of Louisville  
55  
56 456 Institutional Animal Care and Use Committee. The levels of *P. gingivalis* colonization were  
57  
58  
59  
60



1  
2  
3 457 determined by qPCR with the *P. gingivalis* 16SrRNA gene as described (Daep *et al.*, 2011). On  
4  
5  
6 458 days 1, 3 and 8 after the last infection, mice were euthanized and the upper and lower jaw with  
7  
8 459 gingival tissue were recovered. After RNA extraction, the ratio of ZEB1 mRNA to GAPDH mRNA  
9  
10  
11 460 for each mouse was determined by qRT-PCR using the 2- $\Delta$ CT method.  
12  
13  
14 461

15  
16 462 **Human oral tissue immunofluorescent and immunohistochemical staining**  
17

18 463 Paraffin embedded human tongue biopsy samples were sectioned at 4  $\mu$ m, dewaxed and  
19  
20  
21 464 rehydrated. The slides were blocked with 10% goat serum for 1 h, and reacted with *P. gingivalis*  
22  
23 465 33277 or *S. gordonii* antibodies 1:1000 for 2 h at room temperature. Secondary Alexa Fluor 488  
24  
25 466 conjugated anti-rabbit antibody (1:500) was for 1 h, following which slides were treated with  
26  
27  
28 467 DAPI (1:2000). Slides were mounted with VectaShield (Vector Labs, Burlingame, CA) and imaged  
29  
30  
31 468 with a Zeiss Axiocam MRc5 fluorescence microscope. Procedures were approved by the  
32  
33 469 University of Louisville Institutional Review Board.  
34  
35

36 470  
37  
38 471 **Statistical analyses**  
39

40  
41 472 Statistical analyses were conducted using the GraphPad Prism software. Data were evaluated  
42  
43 473 by one-way ANOVA with Tukey's multiple comparison test. Experimental data presented are  
44  
45 474 representative of at least three biological replicates.  
46  
47

48 475  
49  
50  
51 476 **Acknowledgements**  
52

53 477 We thank the NIH/NIDCR for support through DE011111, DE017921, DE016690 and DE023193.  
54  
55  
56 478

479 **Conflict of Interest**

480 The authors have no conflict of interest to declare.

For Peer Review

References

Baud, J., Varon, C., Chabas, S., Chambonnier, L., Darfeuille, F., and Staedel, C. (2013) *Helicobacter pylori* initiates a mesenchymal transition through ZEB1 in gastric epithelial cells. *PLoS One* **8**: e60315.

Bedal, K.B., Grassel, S., Oefner, P.J., Reinders, J., Reichert, T.E., and Bauer, R. (2014) Collagen XVI induces expression of MMP9 via modulation of AP-1 transcription factors and facilitates invasion of oral squamous cell carcinoma. *PLoS One* **9**: e86777.

Belton, C.M., Izutsu, K.T., Goodwin, P.C., Park, Y., and Lamont, R.J. (1999) Fluorescence image analysis of the association between *Porphyromonas gingivalis* and gingival epithelial cells. *Cell Microbiol* **1**: 215-223.

Benitez-Paez, A., Belda-Ferre, P., Simon-Soro, A., and Mira, A. (2014) Microbiota diversity and gene expression dynamics in human oral biofilms. *BMC Genomics* **15**: 311.

Bessede, E., Staedel, C., Acuna Amador, L.A., Nguyen, P.H., Chambonnier, L., Hatakeyama, M., et al. (2014) *Helicobacter pylori* generates cells with cancer stem cell properties via epithelial-mesenchymal transition-like changes. *Oncogene* **33**: 4123-4131.

Bosshardt, D.D., and Lang, N.P. (2005) The junctional epithelium: from health to disease. *J Dent Res* **84**: 9-20.

Bostanci, N., and Belibasakis, G.N. (2012) *Porphyromonas gingivalis*: an invasive and evasive opportunistic oral pathogen. *FEMS Microbiol Lett* **333**: 1-9.

Brabletz, S., and Brabletz, T. (2010) The ZEB/miR-200 feedback loop--a motor of cellular plasticity in development and cancer? *EMBO Rep* **11**: 670-677.

Castellarin, M., Warren, R.L., Freeman, J.D., Dreolini, L., Krzywinski, M., Strauss, J., et al. (2012) *Fusobacterium nucleatum* infection is prevalent in human colorectal carcinoma. *Genome Res* **22**: 299-306.

Daep, C.A., Novak, E.A., Lamont, R.J., and Demuth, D.R. (2011) Structural dissection and in vivo effectiveness of a peptide inhibitor of *Porphyromonas gingivalis* adherence to *Streptococcus gordonii*. *Infect Immun* **79**: 67-74.

Enersen, M., Nakano, K., and Amano, A. (2013) *Porphyromonas gingivalis* fimbriae. *J Oral Microbiol* **5**: 10.3402.

Gallimidi, A.B., Fischman, S., Revach, B., Bulvik, R., Maliutina, A., Rubinstein, A.M., et al. (2015) Periodontal pathogens *Porphyromonas gingivalis* and *Fusobacterium nucleatum* promote tumor progression in an oral-specific chemical carcinogenesis model. *Oncotarget* **6**: 22613-22623.

Garrett, W.S. (2015) Cancer and the microbiota. *Science* **348**: 80-86.

Gheldof, A., Hulpiau, P., van Roy, F., De Craene, B., and Berx, G. (2012) Evolutionary functional analysis and molecular regulation of the ZEB transcription factors. *Cell Mol Life Sci* **69**: 2527-2541.

Gur, C., Ibrahim, Y., Isaacson, B., Yamin, R., Abed, J., Gamliel, M., et al. (2015) Binding of the Fap2 protein of *Fusobacterium nucleatum* to human inhibitory receptor TIGIT protects tumors from immune cell attack. *Immunity* **42**: 344-355.

Hajishengallis, G. (2014) The inflammophilic character of the periodontitis-associated microbiota. *Mol Oral Microbiol* **29**: 248-257.

- Hajishengallis, G., Krauss, J.L., Liang, S., McIntosh, M.L., and Lambris, J.D. (2012) Pathogenic microbes and community service through manipulation of innate immunity. *Adv Exp Med Biol* **946**: 69-85.
- Hajishengallis, G., Lamont, R.J., and Graves, D.T. (2015) The enduring importance of animal models in understanding periodontal disease. *Virulence* **6**: 229-235.
- Handfield, M., Mans, J.J., Zheng, G., Lopez, M.C., Mao, S., Progulske-Fox, A., *et al.* (2005) Distinct transcriptional profiles characterize oral epithelium-microbiota interactions. *Cell Microbiol* **7**: 811-823.
- Hendrickson, E.L., Wang, T., Beck, D.A., Dickinson, B.C., Wright, C.J., Lamont, R.J., and Hackett, M. (2014) Proteomics of *Fusobacterium nucleatum* within a model developing oral microbial community. *Microbiologyopen* **3**: 729-751.
- Heymann, R., Wroblewski, J., Terling, C., Midtvedt, T., and Obrink, B. (2001) The characteristic cellular organization and CEACAM1 expression in the junctional epithelium of rats and mice are genetically programmed and not influenced by the bacterial microflora. *J Periodontol* **72**: 454-460.
- Inaba, H., Sugita, H., Kuboniwa, M., Iwai, S., Hamada, M., Noda, T., *et al.* (2014) *Porphyromonas gingivalis* promotes invasion of oral squamous cell carcinoma through induction of proMMP9 and its activation. *Cell Microbiol* **16**: 131-145.
- Jemal, A., Siegel, R., Ward, E., Hao, Y., Xu, J., Murray, T., and Thun, M.J. (2008) Cancer statistics, 2008. *CA Cancer J Clin* **58**: 71-96.
- Jia, B., Liu, H., Kong, Q., and Li, B. (2012) Overexpression of ZEB1 associated with metastasis and invasion in patients with gastric carcinoma. *Mol Cell Biochem* **366**: 223-229.
- Kamarajan, P., Garcia-Pardo, A., D'Silva, N.J., and Kapila, Y.L. (2010) The CS1 segment of fibronectin is involved in human OSCC pathogenesis by mediating OSCC cell spreading, migration, and invasion. *BMC Cancer* **10**: 330.
- Katz, J., Onate, M.D., Pauley, K.M., Bhattacharyya, I., and Cha, S. (2011) Presence of *Porphyromonas gingivalis* in gingival squamous cell carcinoma. *Int J Oral Sci* **3**: 209-215.
- Khanom, R., Sakamoto, K., Pal, S.K., Shimada, Y., Morita, K., Omura, K., *et al.* (2012) Expression of basal cell keratin 15 and keratin 19 in oral squamous neoplasms represents diverse pathophysiologies. *Histol Histopathol* **27**: 949-959.
- Kim, S.S., Ruiz, V.E., Carroll, J.D., and Moss, S.F. (2011) *Helicobacter pylori* in the pathogenesis of gastric cancer and gastric lymphoma. *Cancer Lett* **305**: 228-238.
- Kostic, A.D., Gevers, D., Pédamallu, C.S., Michaud, M., Duke, F., Earl, A.M., *et al.* (2012) Genomic analysis identifies association of *Fusobacterium* with colorectal carcinoma. *Genome Res* **22**: 292-298.
- Kruger, A., Arlt, M.J., Gerg, M., Kopitz, C., Bernardo, M.M., Chang, M., *et al.* (2005) Antimetastatic activity of a novel mechanism-based gelatinase inhibitor. *Cancer Res* **65**: 3523-3526.
- Kuboniwa, M., Hasegawa, Y., Mao, S., Shizukuishi, S., Amano, A., Lamont, R.J., and Yilmaz, O. (2008) *P. gingivalis* accelerates gingival epithelial cell progression through the cell cycle. *Microbes Infect* **10**: 122-128.
- Lamont, R.J., Chan, A., Belton, C.M., Izutsu, K.T., Vasel, D., and Weinberg, A. (1995) *Porphyromonas gingivalis* invasion of gingival epithelial cells. *Infect Immun* **63**: 3878-3885.

Lamont, R.J., and Hajishengallis, G. (2015) Polymicrobial synergy and dysbiosis in inflammatory disease. *Trends Mol Med* **21**: 172-183.

Lamont, R.J., and Jenkinson, H.F. (1998) Life below the gum line: pathogenic mechanisms of *Porphyromonas gingivalis*. *Microbiol Mol Biol Rev* **62**: 1244-1263.

Lamouille, S., Xu, J., and Derynck, R. (2014) Molecular mechanisms of epithelial-mesenchymal transition. *Nat Rev Mol Cell Biol* **15**: 178-196.

Lee, C.H., Chang, J.S., Syu, S.H., Wong, T.S., Chan, J.Y., Tang, Y.C., *et al.* (2015) IL-1beta promotes malignant transformation and tumor aggressiveness in oral cancer. *J Cell Physiol* **230**: 875-884.

Liu, Y., Costantino, M.E., Montoya-Durango, D., Higashi, Y., Darling, D.S., and Dean, D.C. (2007) The zinc finger transcription factor ZFX1A is linked to cell proliferation by Rb-E2F1. *Biochem J* **408**: 79-85.

Manavella, P.A., Roqueiro, G., Darling, D.S., and Cabanillas, A.M. (2007) The ZFX1A gene is differentially autoregulated by its isoforms. *Biochem Biophys Res Commun* **360**: 621-626.

Mao, S., Park, Y., Hasegawa, Y., Tribble, G.D., James, C.E., Handfield, M., *et al.* (2007) Intrinsic apoptotic pathways of gingival epithelial cells modulated by *Porphyromonas gingivalis*. *Cell Microbiol* **9**: 1997-2007.

Michaud, D.S. (2013) Role of bacterial infections in pancreatic cancer. *Carcinogenesis* **34**: 2193-2197.

Moffatt-Jauregui, C.E., Robinson, B., de Moya, A.V., Brockman, R.D., Roman, A.V., Cash, M.N., *et al.* (2013) Establishment and characterization of a telomerase immortalized human gingival epithelial cell line. *J Periodontal Res* **48**: 713-721.

Moffatt, C.E., and Lamont, R.J. (2011) *Porphyromonas gingivalis* induction of microRNA-203 expression controls suppressor of cytokine signaling 3 in gingival epithelial cells. *Infect Immun* **79**: 2632-2637.

Nadkarni, M.A., Chhour, K.L., Chapple, C.C., Nguyen, K.A., and Hunter, N. (2014) The profile of *Porphyromonas gingivalis* *kgp* biotype and *fimA* genotype mosaic in subgingival plaque samples. *FEMS Microbiol Lett* **361**: 190-194.

Nagy, K.N., Sonkodi, I., Szoke, I., Nagy, E., and Newman, H.N. (1998) The microflora associated with human oral carcinomas. *Oral Oncol* **34**: 304-308.

Naito, M., Hirakawa, H., Yamashita, A., Ohara, N., Shoji, M., Yukitake, H., *et al.* (2008) Determination of the genome sequence of *Porphyromonas gingivalis* strain ATCC 33277 and genomic comparison with strain W83 revealed extensive genome rearrangements in *P. gingivalis*. *DNA Res* **15**: 215-225.

Nishikawa, K., and Duncan, M.J. (2010) Histidine kinase-mediated production and autoassembly of *Porphyromonas gingivalis* fimbriae. *J Bacteriol* **192**: 1975-1987.

Rubinstein, M.R., Wang, X., Liu, W., Hao, Y., Cai, G., and Han, Y.W. (2013) *Fusobacterium nucleatum* promotes colorectal carcinogenesis by modulating E-cadherin/beta-catenin signaling via its FadA adhesin. *Cell Host Microbe* **14**: 195-206.

Sahingur, S.E., and Yeudall, W.A. (2015) Chemokine function in periodontal disease and oral cavity cancer. *Front Immunol* **6**: 214.

- Sanchez-Tillo, E., Liu, Y., de Barrios, O., Siles, L., Fanlo, L., Cuatrecasas, M., *et al.* (2012) EMT-activating transcription factors in cancer: beyond EMT and tumor invasiveness. *Cell Mol Life Sci* **69**: 3429-3456.
- Sawant, S.S., Vaidya, M., Chaukar, D.A., Alam, H., Dmello, C., Gangadaran, P., *et al.* (2014) Clinical significance of aberrant vimentin expression in oral premalignant lesions and carcinomas. *Oral Dis* **20**: 453-465.
- Scanlon, C.S., Van Tubergen, E.A., Inglehart, R.C., and D'Silva, N.J. (2013) Biomarkers of epithelial-mesenchymal transition in squamous cell carcinoma. *J Dent Res* **92**: 114-121.
- Takeuchi, H., Hirano, T., Whitmore, S.E., Morisaki, I., Amano, A., and Lamont, R.J. (2013) The serine phosphatase SerB of *Porphyromonas gingivalis* suppresses IL-8 production by dephosphorylation of NF-kappaB RelA/p65. *PLoS Pathog* **9**: e1003326.
- Tribble, G.D., Kerr, J.E., and Wang, B.Y. (2013) Genetic diversity in the oral pathogen *Porphyromonas gingivalis*: molecular mechanisms and biological consequences. *Future Microbiol* **8**: 607-620.
- Tribble, G.D., Lamont, G.J., Progulske-Fox, A., and Lamont, R.J. (2007) Conjugal transfer of chromosomal DNA contributes to genetic variation in the oral pathogen *Porphyromonas gingivalis*. *J Bacteriol* **189**: 6382-6388.
- Valm, A.M., Mark Welch, J.L., Rieken, C.W., Hasegawa, Y., Sogin, M.L., Oldenbourg, R., *et al.* (2011) Systems-level analysis of microbial community organization through combinatorial labeling and spectral imaging. *Proc Natl Acad Sci U S A* **108**: 4152-4157.
- Vandewalle, C., Van Roy, F., and Berx, G. (2009) The role of the ZEB family of transcription factors in development and disease. *Cell Mol Life Sci* **66**: 773-787.
- Watanabe, K., Yilmaz, O., Nakhjiri, S.F., Belton, C.M., and Lamont, R.J. (2001) Association of mitogen-activated protein kinase pathways with gingival epithelial cell responses to *Porphyromonas gingivalis* infection. *Infect Immun* **69**: 6731-6737.
- Westermarck, J., and Kahari, V.M. (1999) Regulation of matrix metalloproteinase expression in tumor invasion. *FASEB J* **13**: 781-792.
- Whitmore, S.E., and Lamont, R.J. (2014) Oral bacteria and cancer. *PLoS Pathog* **10**: e1003933.
- Wikner, J., Grobe, A., Pantel, K., and Riethdorf, S. (2014) Squamous cell carcinoma of the oral cavity and circulating tumour cells. *World J Clin Oncol* **5**: 114-124.
- Wright, C.J., Burns, L.H., Jack, A.A., Back, C.R., Dutton, L.C., Nobbs, A.H., *et al.* (2013) Microbial interactions in building of communities. *Mol Oral Microbiol* **28**: 83-101.
- Wright, C.J., Xue, P., Hirano, T., Liu, C., Whitmore, S.E., Hackett, M., and Lamont, R.J. (2014) Characterization of a bacterial tyrosine kinase in *Porphyromonas gingivalis* involved in polymicrobial synergy. *Microbiologyopen* **3**: 383-394.
- Yang, G., Yuan, J., and Li, K. (2013) EMT transcription factors: implication in osteosarcoma. *Med Oncol* **30**: 697.
- Yilmaz, O., Jungas, T., Verbeke, P., and Ojcius, D.M. (2004) Activation of the phosphatidylinositol 3-kinase/Akt pathway contributes to survival of primary epithelial cells infected with the periodontal pathogen *Porphyromonas gingivalis*. *Infect Immun* **72**: 3743-3751.
- Yilmaz, O., Verbeke, P., Lamont, R.J., and Ojcius, D.M. (2006) Intercellular spreading of *Porphyromonas gingivalis* infection in primary gingival epithelial cells. *Infect Immun* **74**: 703-710.

Zhang, P., Cai, Y., Soofi, A., and Dressler, G.R. (2012) Activation of Wnt11 by transforming growth factor-beta drives mesenchymal gene expression through non-canonical Wnt protein signaling in renal epithelial cells. *J Biol Chem* **287**: 21290-21302.

Zhang, P., Wei, Y., Wang, L., Debeb, B.G., Yuan, Y., Zhang, J., *et al.* (2014) ATM-mediated stabilization of ZEB1 promotes DNA damage response and radioresistance through CHK1. *Nat Cell Biol* **16**: 864-875.

Zhao, D., Tang, X.F., Yang, K., Liu, J.Y., and Ma, X.R. (2012) Over-expression of integrin-linked kinase correlates with aberrant expression of Snail, E-cadherin and N-cadherin in oral squamous cell carcinoma: implications in tumor progression and metastasis. *Clin Exp Metastasis* **29**: 957-969.

Zhou, Q., and Amar, S. (2007) Identification of signaling pathways in macrophage exposed to *Porphyromonas gingivalis* or to its purified cell wall components. *J Immunol* **179**: 7777-7790.



## Supporting Information

Figure S1. Immunoblot of whole cell lysates of *P. gingivalis* strains probed with polyclonal antibodies to the FimA protein of strain 33277.

Figure S2. JNK knockdown does not affect regulation of Zeb1 by *P. gingivalis*. A. TIGK cells were transiently transfected with siRNA to JNK1/2 (si Jnk, 100 nM, Sigma) or scrambled siRNA (si ctr). Control (ctr) cells were nontransfected. JNK mRNA levels in transfected cells were measured by qRT-PCR. Data were normalized to GAPDH mRNA and are expressed relative to ctr. Results are means  $\pm$  SD, n = 3; \*\*\* P < 0.001. B. Transfected TIGKs cells were infected with *P. gingivalis* 33277 for 24 h at MOI 100. ZEB1 mRNA was measured by qRT-PCR, the data were normalized to GAPDH mRNA and are expressed relative to the noninfected (NI) control. Results are means  $\pm$  SD, n = 3; \*\*\* P < 0.001 compared to NI; NS: not significant.

Figure S3. Pharmacological inhibition of Akt does not affect regulation of Zeb1 by *P. gingivalis*. TIGK cells were preincubated with 10  $\mu$ M LY294002 or vehicle (DMSO) only for 1 h and infected with *P. gingivalis* 33277 MOI 50 or 100 for 6 h. ZEB1 mRNA levels were measured by qRT-PCR, normalized to GAPDH mRNA and are expressed relative to noninfected (NI) controls. Results are means  $\pm$  SD, n = 3; \* P < 0.05; \*\*\* P < 0.001; NS: not significant.

Figure S4. A non-invasive mutant of *P. gingivalis* can induce ZEB1 expression. qRT-PCR of ZEB1 mRNA expression in TIGK cells infected with *P. gingivalis* 33277 (Pg WT) or a  $\Delta$ serB mutant. Data were normalized to GAPDH mRNA and are expressed relative to noninfected (NI) controls. Results are means  $\pm$  SD, n = 3; \*\*\* P < 0.001 compared to NI; NS: not significant.



1  
2  
3  
4  
5  
6  
7  
8  
9  
10  
11  
12  
13  
14  
15  
16  
17  
18  
19  
20  
21  
22  
23  
24  
25  
26  
27  
28  
29  
30  
31  
32  
33  
34  
35  
36  
37  
38  
39  
40  
41  
42  
43  
44  
45  
46  
47  
48  
49  
50  
51  
52  
53  
54  
55  
56  
57  
58  
59  
60

Figure S5. Expression of miRNA-21 is not down-regulated by *P. gingivalis*. TIGK cells were infected with *P. gingivalis* 33277 (Pg) at MOI 100 for the time indicated. miRNA levels were measured by qRT-PCR, normalized to RNU48 miRNA, and expressed relative to noninfected (NI) controls. Results are means  $\pm$  SD, n = 3; \*\*\* P < 0.001 compared to NI.

Figure S6. *P. gingivalis* increases expression of vimentin. Immunoblot of lysates of TIGK cells infected with *P. gingivalis* 33277 for 24 h at the MOI indicated. Control cells were uninfected (NI). Duplicate blots were probed with antibodies to vimentin or GAPDH (loading control).

Figure S7. Colonization of mice. Mice were orally infected with 10<sup>7</sup> cfu *P. gingivalis* five times at 2-days intervals. Bacterial samples were collected along the gingiva of the upper molars. Samples were lysed, DNA extracted and qPCR performed with primers specific for *P. gingivalis* 16S DNA. For enumeration, genomic DNA was isolated from laboratory cultures of *P. gingivalis* 33277 (numbers determined by viable counting) and a series of dilutions prepared. The number of gene copies in the oral samples was determined by comparison with the standard curve. In the sham infected animals, 2 of 5 mice were colonized with low levels of organisms sufficient similar to *P. gingivalis* to give a positive result. *P. gingivalis* levels from day 1, 3 and 8 were statistically greater than sham infected (P < 0.0001) but were not statistically different from each other.

Figure S8. Fluorescent confocal microscopy of a carcinoma in situ biopsy sample probed with *P. gingivalis* antibodies (green) and stained with DAPI (blue). Cells were imaged at magnification x63. Red arrows point to a discrete fluorescent spot, yellow arrows indicate the same position

where that spot is absent. Numbers are the slice number in an optical stack of 40 slices at 0.4  $\mu\text{m}$ . Fluorescent spots are present in typically 5 to 7 adjacent optical slices (0.4  $\mu\text{m}$  slices), indicating that the fluorescent particles are about 2.0 to 2.8  $\mu\text{m}$  in size, consistent with the size of *P. gingivalis*.

For Peer Review

**Figure legends**

Figure 1. *P. gingivalis* up-regulates ZEB1 expression in TIGK cells in a FimA-dependent manner.

A. TIGKs were infected with *P. gingivalis* 33277 at the MOI and time indicated. ZEB1 mRNA levels were measured by qRT-PCR. Data were normalized to GAPDH mRNA and are expressed relative to noninfected (NI) controls. Results are means  $\pm$  SD; n = 3; \* P < 0.05; \*\*\* P < 0.001.

B. Immunoblot of lysates of TIGK cells infected with *P. gingivalis* 33277 for 24 h at the MOI indicated. Control cells were uninfected (NI). Duplicate blots were probed with antibodies to ZEB1 or GAPDH (loading control).

C. ZEB1 mRNA levels in TIGKs after 72 h infection with *P. gingivalis* 33277 at MOI indicated. qRT-PCR data were normalized to GAPDH mRNA and are expressed relative to noninfected (NI) controls. Results are means  $\pm$  SD, n = 3; \*\* P < 0.01; \*\*\* P < 0.001.

D. Fluorescent confocal microscopy of TIGK cells infected with *P. gingivalis* 33277 (Pg) at MOI 50 or MOI 100 for 24 h. Control cells were noninfected (NI). Cells were fixed and probed with ZEB1 antibodies (green). Actin (red) was stained with Texas Red-phalloidin, and nuclei (blue) stained with DAPI. Cells were imaged at magnification x63, and shown are representative merged images of projections of z-stacks obtained with Volocity software. Bar = 10  $\mu$ m.

E. Nuclear localization of ZEB1 calculated by Pearson's correlation coefficient from images in C (n=100 cells) using Volocity software. Results are mean  $\pm$  SD; \*\* P < 0.01; \*\*\* P < 0.001.

F. qRT-PCR of ZEB1 mRNA expression in TIGK cells infected with *P. gingivalis* (Pg) strains at MOI 100 for 24 h. qRT-PCR data were normalized to GAPDH mRNA and are expressed relative to noninfected (NI) controls. Results are means  $\pm$  SD, n = 3; \* P < 0.05; \*\*\* P < 0.001.

G. qRT-PCR of ZEB1 mRNA expression in TIGK cells infected with *P. gingivalis* 33277 (Pg WT),  $\Delta fimA$  mutant, or W83, or Pg WT in the presence of membrane insert. qRT-PCR data were normalized to GAPDH mRNA and are expressed relative to noninfected (NI) controls. Results are means  $\pm$  SD, n = 3; \*\*\* P < 0.001 compared to NI; ### P < 0.001 compared to Pg WT.

Figure 2. *P. gingivalis* communities regulate ZEB1 expression.

A. qRT-PCR of ZEB1 mRNA expression in TIGK cells infected with *P. gingivalis* 33277 (Pg), *S. gordonii* (Sg) or a combination of Pg and Sg at MOI 100 for 24 h.

B. qRT-PCR of ZEB1 mRNA expression in TIGK cells infected with *P. gingivalis* 33277 (Pg), *F. nucleatum* (Fn) or a combination of Pg and Fn at MOI 100 for 24 h.

Data were normalized to GAPDH mRNA and are expressed relative to noninfected (NI) controls.

Results are means  $\pm$  SD; n = 3; \*\* P < 0.01; \*\*\* P < 0.001.

Figure 3. *P. gingivalis* regulates ZEB1 promoter activity and increases in ZEB1 levels are not dependent on the miRNA 200 family.

A. TIGK cells were transiently transfected with ZEB1 promoter-luciferase plasmids: Z1p 1000-Luc (-912 bp to +43 bp), Z1p.400-Luc (-367 bp to +43 bp) or Z1p.196-Luc (-212 bp to +43 bp); or with a constitutively-expressing Renilla luciferase reporter. Transfected cells were infected with *P. gingivalis* 33277 (Pg) at MOI 100 for 24 h. Control cells were noninfected (Ctr). Luciferase activity was normalized to the level of Renilla luciferase. Results are mean  $\pm$  SD, n = 3; \* P < 0.01; \*\*\* P < 0.001.

B-D. Expression of mature miRNA-200b (B), miRNA-200c (C), or miRNA-205 (D) in TIGK cells infected with *P. gingivalis* 33277 MOI 100 for the times indicated. miRNA levels were measured by qRT-PCR, normalized to RNU48 miRNA, and expressed relative to noninfected (NI) controls. Results are means  $\pm$  SD, n = 3; \* P < 0.05; \*\* P < 0.01; \*\*\* P < 0.001.

Figure 4. *P. gingivalis* induces MMP9 expression in a FimA-dependent manner.

TIGKs were infected with *P. gingivalis* 33277 (WT) or  $\Delta$ fimA mutant at MOI 10 for 24 h, or left uninfected. A. Culture supernatants were analyzed for MMP9 and MMP2 by gelatin zymography. B. Quantitative analysis of 4 independent zymograms using ImageJ. \* P < 0.05; \*\*\* P < 0.001.

Figure 5. ZEB1 knockdown suppresses TIGK responses to *P. gingivalis*.

A. TIGK cells were transiently transfected with siRNA to ZEB1 (si Zeb1) or scrambled siRNA (si ctr). Control (ctr) cells were nontransfected. ZEB1 mRNA levels in transfected cells were measured by qRT-PCR. Data were normalized to GAPDH mRNA and are expressed relative to ctr. Results are means  $\pm$  SD, n = 3; \*\*\* P < 0.001.

B. Immunoblot of lysates of TIGK cells transfected (as in A) and probed with antibodies to ZEB1 or GAPDH (loading control).

C-D. Transfected TIGK cells (as in A) were infected with *P. gingivalis* 33277 for 24 h at the MOI indicated. The Effect of ZEB1 knockdown on expression of vimentin (B) and MMP9 (C) was measured by qRT-PCR. Data were normalized to GAPDH mRNA and are expressed relative to

the noninfected (NI) control. Results are means  $\pm$  SD, n = 3; \* P < 0.05; \*\* P < 0.01; \*\*\* P < 0.001 compared to NI. #### P < 0.001 compared to si ctr.

Figure 6. *P. gingivalis* increases TIGK migration in a ZEB1-dependent manner.

Quantitative analysis of TIGK migration through matrigel-coated transwells. TIGK cells were transiently transfected with siRNA to ZEB1 (si Zeb1) or scrambled siRNA (si ctr). Control cells were nontransfected. TIGKs were infected with *P. gingivalis* 33277 for 24 h at the MOI indicated. Data are presented as the average number of cells invading through inserts coated with matrigel. Results are means  $\pm$  SD, n = 3; \*\*\* P < 0.001 compared to NI. #### P < 0.001 compared to si ctr.

Figure 7. *P. gingivalis* induces ZEB1 expression in vivo.

A. qRT-PCR of ZEB1 mRNA expression relative to GAPDH control in gingival tissues from mice infected with *P. gingivalis* or sham infected (NI). Tissue samples were collected at days 1, 3 and 8 after infection. Each point represents the determination from a single animal. \* P < 0.05; \*\* P < 0.01.

Figure 8. *P. gingivalis* antigens are present in OSCC.

Tissue biopsy of (A) poorly differentiated carcinoma, and (B) a tongue carcinoma in situ. Bioscopy sections were stained with H&E, *P. gingivalis* 33277 antibodies (Anti-Pg 1:1000) or *S. gordonii* antibodies (Anti-Sg 1:1000) in the presence or absence of DAPI. Controls had no primary

1  
2  
3  
4  
5  
6  
7  
8  
9  
10  
11  
12  
13  
14  
15  
16  
17  
18  
19  
20  
21  
22  
23  
24  
25  
26  
27  
28  
29  
30  
31  
32  
33  
34  
35  
36  
37  
38  
39  
40  
41  
42  
43  
44  
45  
46  
47  
48  
49  
50  
51  
52  
53  
54  
55  
56  
57  
58  
59  
60

antibody. Red blood cells in the connective tissue are autofluorescent. Samples were imaged with a Zeiss AxioCam MRc5 fluorescence microscope at the magnification indicated.

For Peer Review

Table 1. Changes in expression of mesenchymal and epithelial markers in TIGK cells infected with *P. gingivalis* 33277.

		Fold change induced by <i>P. gingivalis</i> 33277	
		MOI 50	MOI 100
Mesenchymal markers	Vimentin	1.72 ± 0.14 **	3.4 ± 0.41 **
	ITGA5	1.06 ± 0.12	1.29 ± 0.23
	MMP-9	8.943 ± 0.38 ***	12.77 ± 0.75 ***
	Fibronectin	1.16 ± 0.05	3.13 ± 0.16 ***
	N-cadherin	2.55 ± 0.34**	2.4 ± 0.17**
Epithelial markers	KRT7	0.97 ± 0.09	1.29 ± 0.09
	KRT19	1.2 ± 0.07	0.63 ± 0.003 ***
	COL-1A1	0.63 ± 0.06 **	0.67 ± 0.035 ***

Data represent qRT-PCR results of the individual genes normalized to that of GAPDH mRNA and expressed relative to noninfected cells. Results are means ± SD, n = 6; \*\* P < 0.01; \*\*\* P < 0.001



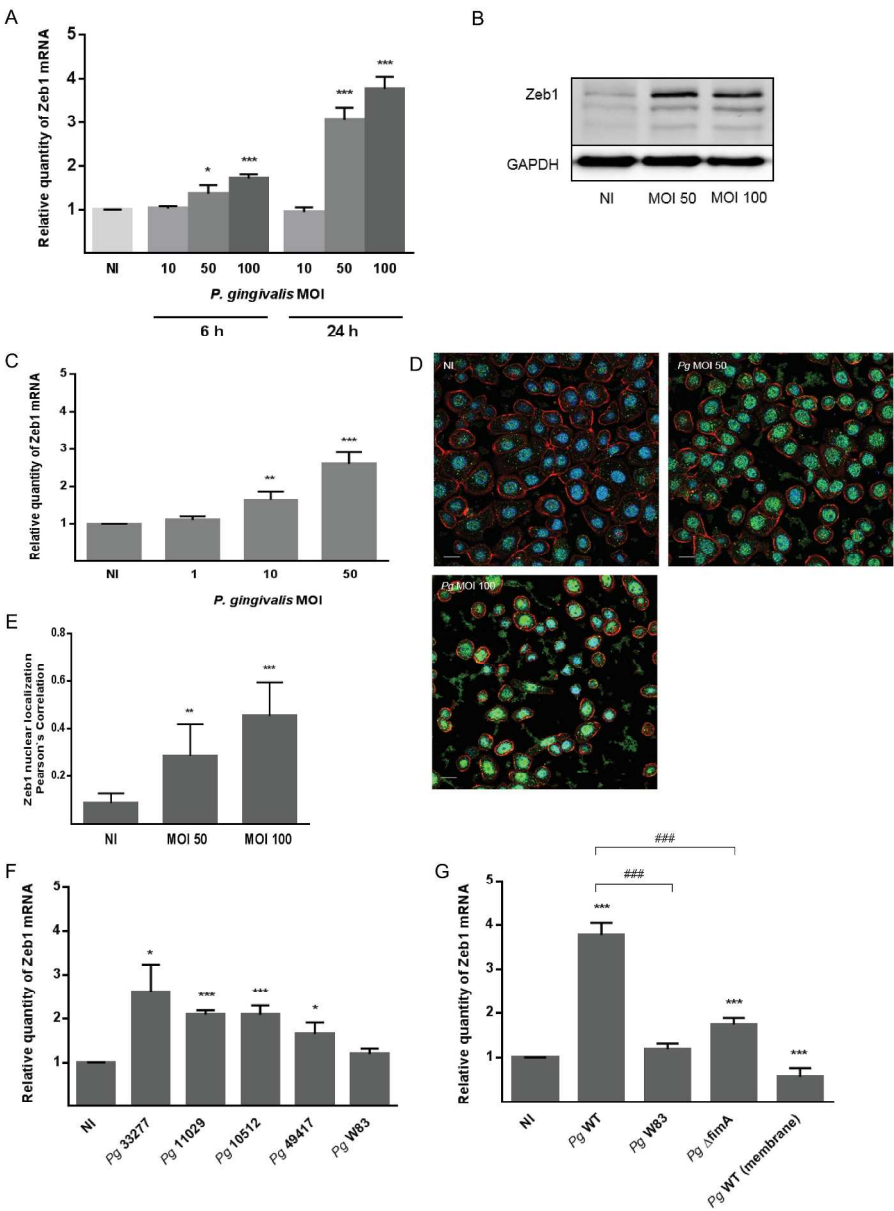


Figure 1. *P. gingivalis* up-regulates ZEB1 expression in TIGK cells in a FimA-dependent manner.

A. TIGKs were infected with *P. gingivalis* 33277 at the MOI and time indicated. ZEB1 mRNA levels were measured by qRT-PCR. Data were normalized to GAPDH mRNA and are expressed relative to noninfected (NI) controls. B. Immunoblot of lysates of TIGK cells infected with *P. gingivalis* 33277 for 24 h at the MOI indicated. Control cells were uninfected (NI). Duplicate blots were probed with antibodies to ZEB1 or GAPDH (loading control). C. ZEB1 mRNA levels in TIGKs after 72 h infection with *P. gingivalis* 33277 at MOI indicated. qRT-PCR data were normalized to GAPDH mRNA and are expressed relative to noninfected (NI) controls. D. Fluorescent confocal microscopy of TIGK cells infected with *P. gingivalis* 33277 (Pg) at MOI 50 or MOI 100 for 24 h. Control cells were noninfected (NI). Cells were fixed and probed with ZEB1 antibodies (green). Actin (red) was stained with Texas Red-phalloidin, and nuclei (blue) stained with DAPI. Cells were imaged at magnification x63, and shown are representative merged images of projections of z-stacks obtained with Volocity software. Bar = 10  $\mu$ m. E. Nuclear localization of ZEB1 calculated by Pearson's correlation coefficient from images in C (n=100 cells) using Volocity software. F. qRT-PCR of ZEB1 mRNA

expression in TIGK cells infected with *P. gingivalis* (Pg) strains at MOI 100 for 24 h. qRT-PCR data were normalized to GAPDH mRNA and are expressed relative to noninfected (NI) controls. G. qRT-PCR of ZEB1 mRNA expression in TIGK cells infected with *P. gingivalis* 33277 (Pg WT),  $\Delta$ fimA mutant, or W83, or Pg WT in the presence of membrane insert. qRT-PCR data were normalized to GAPDH mRNA and are expressed relative to noninfected (NI) controls. Results are means  $\pm$  SD, n = 3; \*\*\* P < 0.001 compared to NI; ### P < 0.001 compared to Pg WT.

259x346mm (300 x 300 DPI)

For Peer Review

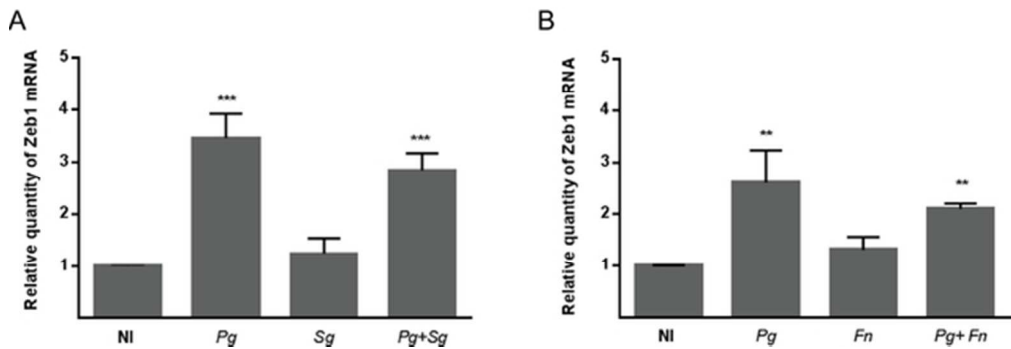


Figure 2. *P. gingivalis* communities regulate ZEB1 expression.  
A. qRT-PCR of ZEB1 mRNA expression in TIGK cells infected with *P. gingivalis* 33277 (Pg), *S. gordonii* (Sg) or a combination of Pg and Sg at MOI 100 for 24 h.  
B. qRT-PCR of ZEB1 mRNA expression in TIGK cells infected with *P. gingivalis* 33277 (Pg), *F. nucleatum* (Fn) or a combination of Pg and Fn at MOI 100 for 24 h.  
Data were normalized to GAPDH mRNA and are expressed relative to noninfected (NI) controls. Results are means  $\pm$  SD; n = 3; \*\* P < 0.01; \*\*\* P < 0.001.

53x18mm (300 x 300 DPI)

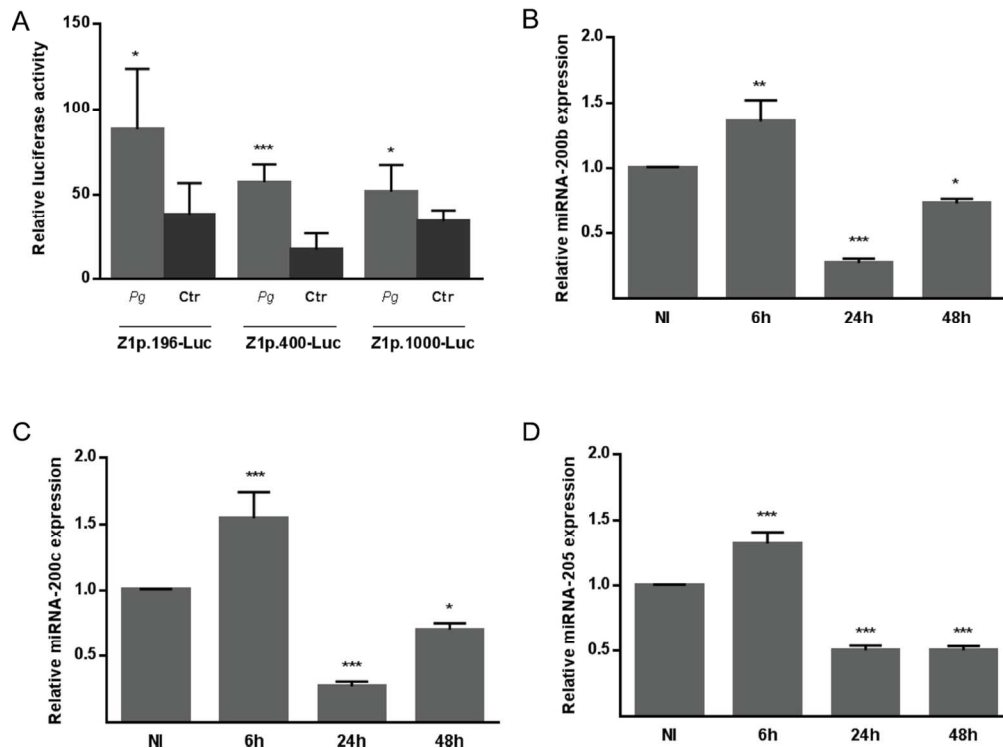


Figure 3. *P. gingivalis* regulates ZEB1 promoter activity and increases in ZEB1 levels are not dependent on the miRNA 200 family.

A. TIGK cells were transiently transfected with ZEB1 promoter-luciferase plasmids: Z1p 1000-Luc (-912 bp to +43 bp), Z1p.400-Luc (-367 bp to +43 bp) or Z1p.196-Luc (-212 bp to +43 bp); or with a constitutively-expressing Renilla luciferase reporter. Transfected cells were infected with *P. gingivalis* 33277 (Pg) at MOI 100 for 24 h. Control cells were noninfected (Ctr). Luciferase activity was normalized to the level of Renilla luciferase. Results are mean  $\pm$  SD,  $n = 3$ ; \*  $P < 0.01$ ; \*\*\*  $P < 0.001$ . B-D. Expression of mature miRNA-200b (B), miRNA-200c (C), or miRNA-205 (D) in TIGK cells infected with *P. gingivalis* 33277 MOI 100 for the times indicated. miRNA levels were measured by qRT-PCR, normalized to RNU48 miRNA, and expressed relative to noninfected (NI) controls. Results are means  $\pm$  SD,  $n = 3$ ; \*  $P < 0.05$ ; \*\*  $P < 0.01$ ; \*\*\*  $P < 0.001$ .

115x85mm (300 x 300 DPI)

1  
2  
3  
4  
5  
6  
7  
8  
9  
10  
11  
12  
13  
14  
15  
16  
17  
18  
19  
20  
21  
22  
23  
24  
25  
26  
27  
28  
29  
30  
31  
32  
33  
34  
35  
36  
37  
38  
39  
40  
41  
42  
43  
44  
45  
46  
47  
48  
49  
50  
51  
52  
53  
54  
55  
56  
57  
58  
59  
60

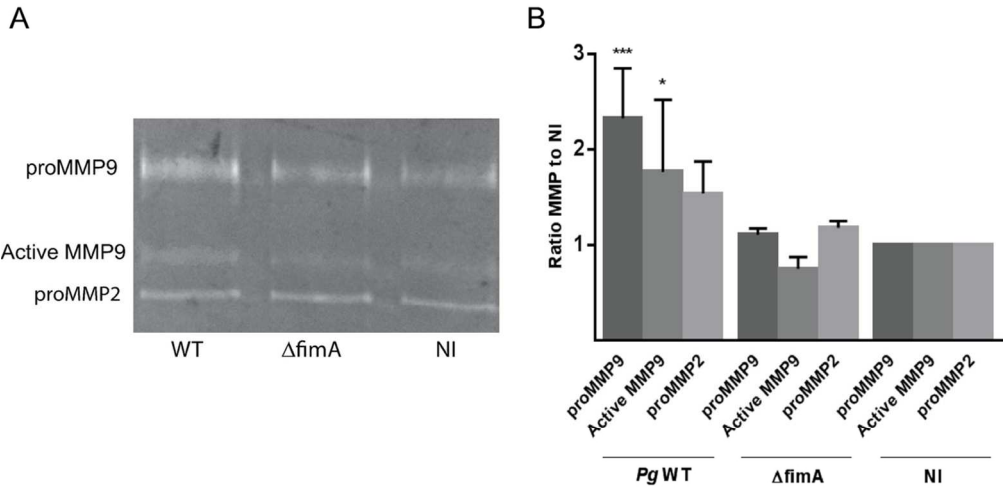


Figure 4. *P. gingivalis* induces MMP9 expression in a FimA-dependent manner. TIGKs were infected with *P. gingivalis* 33277 (WT) or  $\Delta$ fimA mutant at MOI 10 for 24 h, or left uninfected. A. Culture supernatants were analyzed for MMP9 and MMP2 by gelatin zymography. B. Quantitative analysis of 4 independent zymograms using ImageJ. \*  $P < 0.05$ ; \*\*\*  $P < 0.001$ .

106x78mm (300 x 300 DPI)

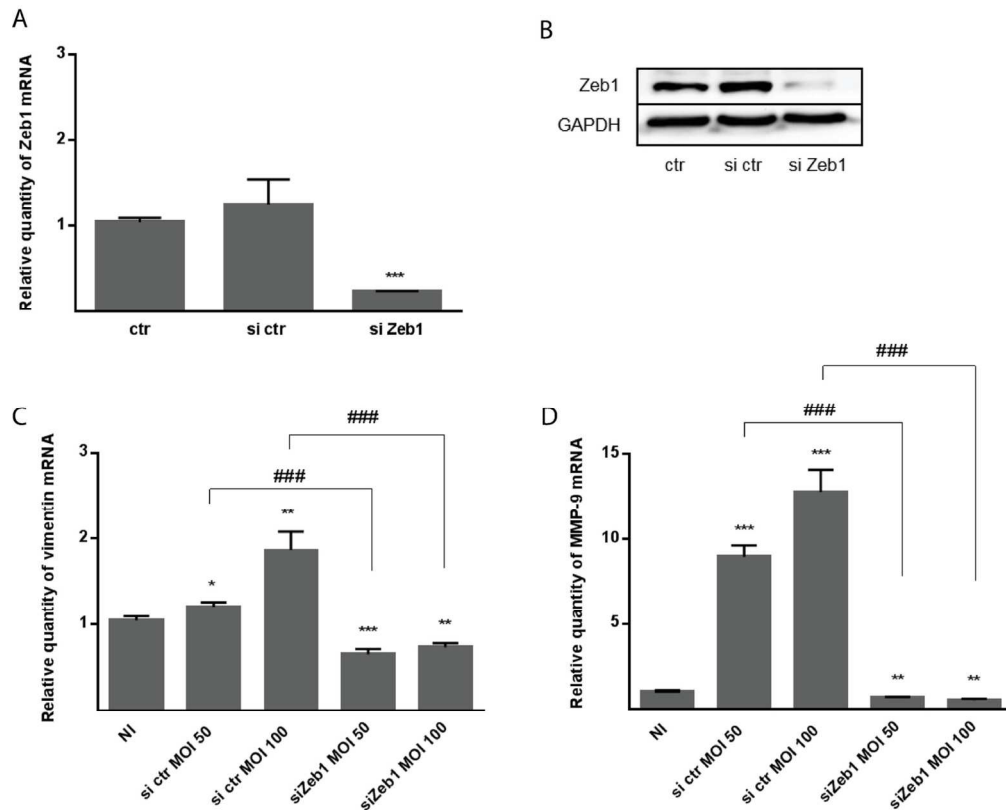


Figure 5. ZEB1 knockdown suppresses TIGK responses to *P. gingivalis*.

A. TIGK cells were transiently transfected with siRNA to ZEB1 (si Zeb1) or scrambled siRNA (si ctr). Control (ctr) cells were nontransfected. ZEB1 mRNA levels in transfected cells were measured by qRT-PCR. Data were normalized to GAPDH mRNA and are expressed relative to ctr. Results are means  $\pm$  SD,  $n = 3$ ; \*\*\*  $P < 0.001$ .

B. Immunoblot of lysates of TIGK cells transfected (as in A) and probed with antibodies to ZEB1 or GAPDH (loading control).

C-D. Transfected TIGK cells (as in A) were infected with *P. gingivalis* 33277 for 24 h at the MOI indicated. The Effect of ZEB1 knockdown on expression of vimentin (B) and MMP9 (C) was measured by qRT-PCR.

Data were normalized to GAPDH mRNA and are expressed relative to the noninfected (NI) control. Results are means  $\pm$  SD,  $n = 3$ ; \*  $P < 0.05$ ; \*\*  $P < 0.01$ ; \*\*\*  $P < 0.001$  compared to NI. ###  $P < 0.001$  compared to si ctr.

128x103mm (300 x 300 DPI)

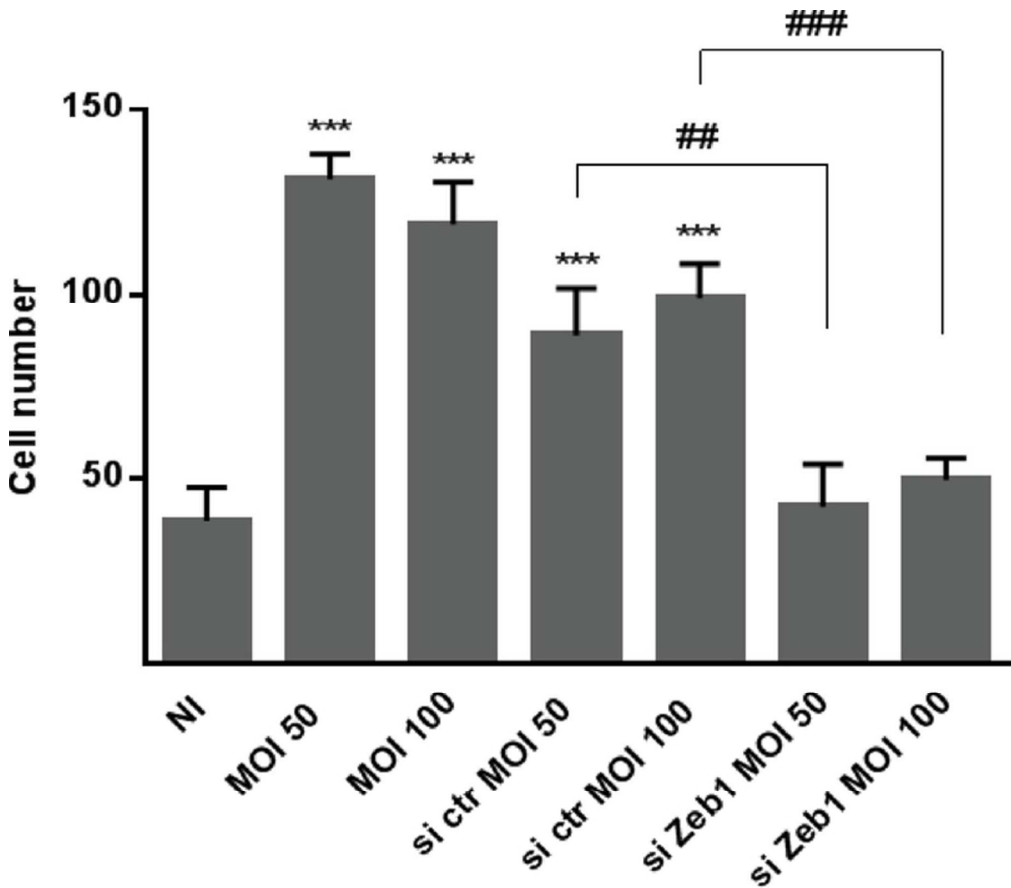


Figure 6. *P. gingivalis* increases TIGK migration in a ZEB1-dependent manner. Quantitative analysis of TIGK migration through matrigel-coated transwells. TIGK cells were transiently transfected with siRNA to ZEB1 (si Zeb1) or scrambled siRNA (si ctr). Control cells were nontransfected. TIGKs were infected with *P. gingivalis* 33277 for 24 h at the MOI indicated. Data are presented as the average number of cells invading through inserts coated with matrigel. Results are means  $\pm$  SD, n = 3; \*\*\* P < 0.001 compared to NI. ### P < 0.001 compared to si ctr.

67x59mm (300 x 300 DPI)

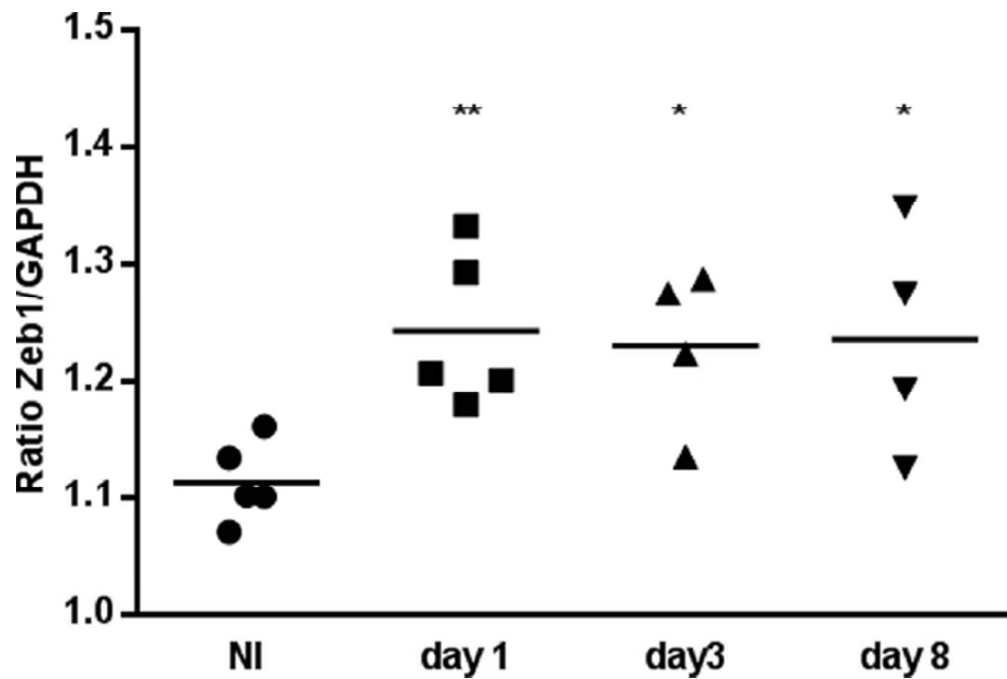


Figure 7. *P. gingivalis* induces ZEB1 expression in vivo.

A. qRT-PCR of ZEB1 mRNA expression relative to GAPDH control in gingival tissues from mice infected with *P. gingivalis* or sham infected (NI). Tissue samples were collected at days 1, 3 and 8 after infection. Each point represents the determination from a single animal. \*  $P < 0.05$ ; \*\*  $P < 0.01$ .

51x34mm (300 x 300 DPI)



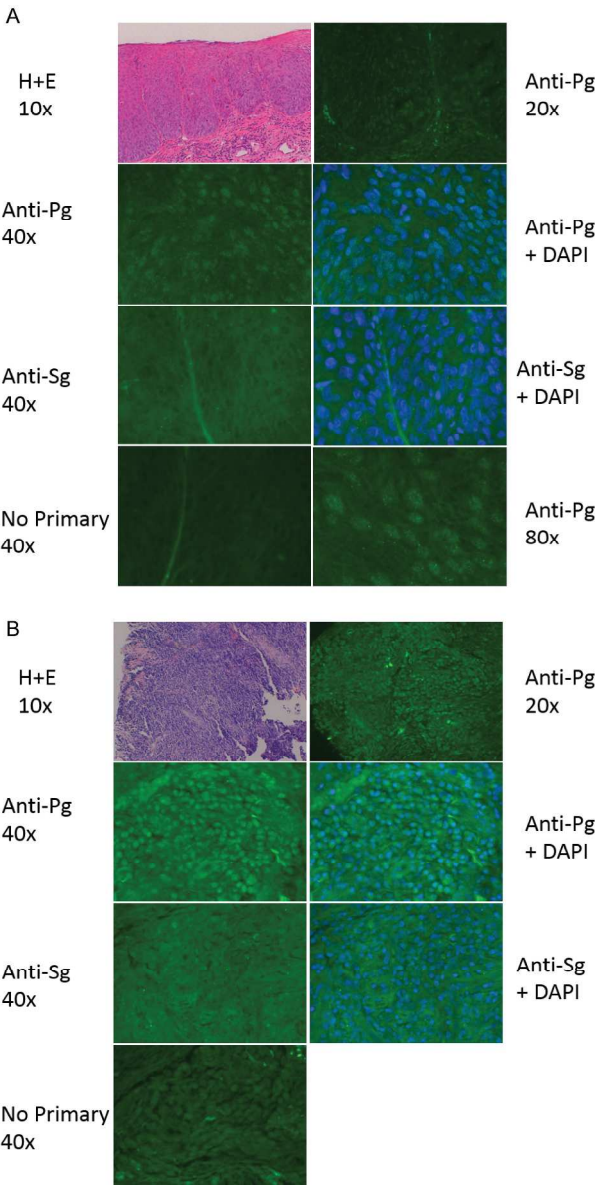


Figure 8. *P. gingivalis* antigens are present in OSCC. Tissue biopsy of (A) poorly differentiated carcinoma, and (B) a tongue carcinoma in situ. Biospsy sections were stained with H&E, *P. gingivalis* 33277 antibodies (Anti-Pg 1:1000) or *S. gordonii* antibodies (Anti-Sg 1:1000) in the presence or absence of DAPI. Controls had no primary antibody. Red blood cells in the connective tissue are autofluorescent. Samples were imaged with a Zeiss Axiocam MRc5 fluorescence microscope at the magnification indicated.

238x280mm (300 x 300 DPI)